



Contents lists available at ScienceDirect

Bioorganic & Medicinal Chemistry

journal homepage: www.elsevier.com/locate/bmc

Novel leucine ureido derivatives as aminopeptidase N inhibitors using click chemistry

Jiangying Cao^a, Chunhua Ma^b, Jie Zang^a, Shuai Gao^a, Qianwen Gao^a, Xiujie Kong^a, Yugang Yan^a, Xuewu Liang^a, Qin'ge Ding^a, Chunlong Zhao^a, Binghe Wang^c, Wenfang Xu^{a,*}, Yingjie Zhang^{a,*}^a Department of Medicinal Chemistry, School of Pharmaceutical Sciences, Shandong University, Jinan 250012, PR China^b School of Chemistry and Chemical Engineering, Henan Normal University, Collaborative Innovation Center of Henan Province for Green Manufacturing of Fine Chemicals, Key Laboratory of Green Chemical Media and Reactions of Ministry of Education, Xinxiang 453007, China^c Department of Chemistry and Center for Diagnostics and Therapeutics, Georgia State University, Atlanta, GA 30303, USA

ARTICLE INFO

Article history:

Received 24 January 2018

Revised 17 April 2018

Accepted 19 April 2018

Available online xxxxx

Keywords:

Aminopeptidase N
CD13

Anti-angiogenesis

Anti-metastasis

Triazole

ABSTRACT

The over-expression of aminopeptidase N on diverse malignant cells is associated with the tumor angiogenesis and metastasis. In this report, one new series of leucine ureido derivatives containing the triazole moiety was designed, synthesized and evaluated as APN inhibitors. Among them, compound **13v** showed the best APN inhibition with an IC₅₀ value of 0.089 ± 0.007 μM, which was two orders of magnitude lower than that of bestatin (IC₅₀ = 9.4 ± 0.5 μM). Compound **13v** also showed dose-dependent anti-angiogenesis activities. Even at the lower concentration (10 μM), compound **13v** presented similar anti-angiogenesis activity compared with bestatin at 100 μM in both the human umbilical vein endothelial cells (HUVECs) capillary tube formation assay and the rat thoracic aorta rings test. Moreover, compared with bestatin, **13v** exhibited comparable, if not better *in vivo* anti-metastasis activity in a mouse H22 pulmonary metastasis model.

© 2018 Published by Elsevier Ltd.

1. Introduction

Aminopeptidase N (APN, CD13) is a zinc-dependent membrane bound exopeptidase, consisting of 967 amino acids with a short cytoplasmic part, a single transmembrane domain and a large extracellular catalytic domain.¹ The enzyme preferentially hydrolyzes basic or neutral amino acid residues from the unsubstituted N-terminals of oligopeptides, such as enkephalins, angiotensins, P-substance, cytokines and others.² As a widely distributed and over-expressed enzyme in malignant cells, it is associated with the growth, invasion and metastasis of diverse cancers.^{3–7} Moreover, documents suggested that APN expression, specially on the endothelium of angiogenic vasculature, could be activated by angiogenic signals and is essential for capillary tube formation.^{8,9} All these findings make APN a promising antitumor target.

Based on their different sources, the APN inhibitors (APNIs) can be divided into the natural products and synthetic compounds. Bestatin (**1**, Fig. 1), isolated from the *Streptomyces oliuoreticuli* by Umezawa et al., is the first reported and only marketed natural dipeptidomimetic inhibitor of APN.¹⁰ After that, many natural

products against APN have been documented, including amastatin¹¹, actinonin¹², phebestin¹³, and lapstatin.¹⁴ Our group has a long-standing interest in the development of synthetic APNIs as antitumor agents^{15–21}, among which the leucine ureido-based APNIs (**2**, Fig. 1) exhibited promising *in vitro* and *in vivo* anti-angiogenesis and anti-metastasis potency.^{18–21} Our previous structure-activity relationship studies revealed that structural modifications of the aryl group of **2** were well tolerated.^{18–21} 1,2,3-triazole, which could be readily obtained by click chemistry, is widely used in various biologically active compounds due to its desirable features in the context of medicinal chemistry.^{22–26} For example, triazoles are stable to acid and basic hydrolysis, redox conditions and metabolic degradation. This heterocycle also has the potential to form hydrogen bonds as well as π stacking interactions. Herein, the 1,2,3-triazole moiety was introduced as the surrogate for the aryl group in compound **2** to get a novel series of leucine ureido-based APNIs (**3**, Fig. 1). All target compounds were synthesized efficiently using click chemistry and all the leucine ureido-based compounds exhibited more potent APN inhibitory activities than the positive control bestatin. The superior APN inhibitory activities of several representative compounds were validated using cell-based APN inhibitory assays. The most potent compound **13v** exhibited promising *in vitro* anti-angiogenesis potency and *in vivo* anti-metastasis

* Corresponding authors.

E-mail address: zhangyingjie@sdu.edu.cn (Y. Zhang).

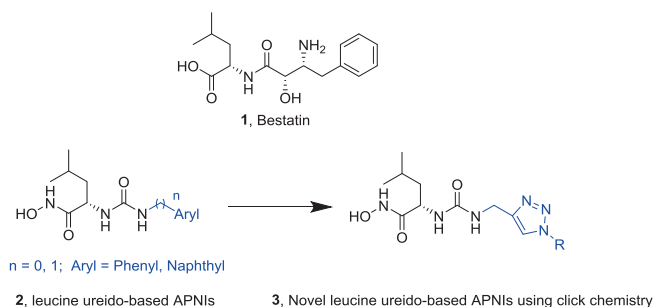


Fig. 1. The design of leucine ureido-based triazole derivatives as APN inhibitors.

potency. Finally, the molecular docking study was used to postulate the binding mode of **13v** in the active site of APN.

2. Chemistry

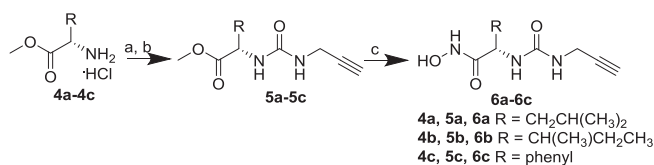
The target compounds were efficiently synthesized following the procedures shown in the Schemes 1–4.

As shown in Scheme 1, compounds **4a–4c** reacted with triphosgene to yield isocyanate, which was then immediately reacted with propargylamine to generate the ureido derivatives **5a–5c**. The ureido derivatives **5a–5c** were converted into key intermediates hydroxamic acids **6a–6c** in the presence of NH_2OK in dry methanol.

As shown in Scheme 2, the aldehydes (**7a–7u**, **7aa–7ff**, **9v–9w**) were converted into their alcohol derivatives (**8a–8u**, **8aa–8ff**, **10v–10w**) via reduction by sodium borohydride in methanol. Compounds **9v–9w** were generated by reaction of **7v–7w** with benzyl bromide. The hydroxyl group of compounds **8a–8u**, **8aa–8ff** and **10v–10w** were converted into a mesyl group under basic conditions and then reacted with sodium azide to yield the azide derivatives (**12a–12w**, **12aa–12ff**). The target compounds **13a–13w** and **13aa–13ff** were prepared by coupling **6a** with compounds **12a–12w** and **12aa–12ff** via click chemistry, respectively. Compounds **14** and **15** were prepared by coupling **6b** with **12a** and **6c** with **12d** via click chemistry, respectively.

Scheme 3 presented the synthesis of compounds **20a–20b**. Compounds **16a–16b** underwent reduction by sodium borohydride to yield compounds **17a–17b**, of which the nitro groups were reduced to amino groups with sodium sulfide. Subsequently, activation of the hydroxyl group with triphenylphosphine in CCl_4/DMF and then reaction with sodium azide led to the azide derivatives **19a–19b**. Compounds **19a–19b** were coupled with **6a** via click chemistry to generate compounds **20a–20b**.

The reactions in Scheme 4 are similar to that of Scheme 2. The aldehydes and ketones (**21a–21h**) underwent reduction to yield the corresponding alcohols (**22a–22h**). Activation of the hydroxyl group followed by nucleophilic substitution led to azide derivatives **24a–24h**, which were coupled with **6a** via click chemistry to yield compounds **25a–25h**, respectively.



Scheme 1. Reagents and conditions: (a) triphosgene, NaHCO_3 , $\text{DCM}/\text{H}_2\text{O}$, ice-bath, 1.5 h; (b) propargylamine, TEA, DCM, 25 °C, 12 h; (c) NH_2OK , MeOH, 25 °C, 0.5 h.

3. Results

The newly synthesized leucine ureido derivatives were firstly evaluated for their enzymatic inhibition using porcine kidney APN (Microsomal, Biocol) with bestatin as the positive control (Table 1). One isoleucine ureido derivative **14** and phenylglycine ureido derivative **15** were also synthesized and evaluated, which exhibited much less potent APN inhibition than their corresponding leucine ureido derivatives **13a** and **13d**, respectively, suggesting that the leucine residue is more suitable for APN recognition. Introduction of various substituents on phenyl group of **13a** led to mono-substituted analogs **13b–13w**, **20a–20b** and multi-substituted analogs **13aa–13ff**. Comparing the mono-substituted analogs, it was found that for chlorine (**13b–13d**), bromine (**13e–13g**), methyl (**13h–13j**), methoxyl (**13k–13m**), ethoxyl (**13s–13u**), benzyloxyl (**13v–13w**) and amino (**20a–20b**) substituted analogs, their APN inhibitory activity order is *ortho*-substituted > *meta*-substituted > *para*-substituted. However, the similar trend was not observed in nitro (**13n–13p**) or cyano (**13q–13r**) substituted analogs. Among multi-substituted analogs **13aa–13ff**, compounds containing two *ortho*-substituents displayed more potent activity than their counterparts with other substitutions patterns (**13aa** vs **13dd**, and **13cc** vs **13ee**). Moreover, compounds containing two *ortho*-substituents are more potent than their counterparts containing one single *ortho*-substituent (**13aa** vs **13b**, **13bb** vs **13h**, and **13cc** vs **13k**). Replacement of the benzyl group of **13a** using other functional groups led to derivatives **25a–25h** with comparable or better APN inhibitory activities to **13a**, indicating that different substituents on the triazole were generally well tolerated. It was worth noting that all our newly synthesized leucine ureido derivatives exhibited better APN inhibitory potency than the positive control bestatin. The most potent compound **13v** ($\text{IC}_{50} = 0.089 \pm 0.007 \mu\text{M}$) was over 100-fold more potent than bestatin ($\text{IC}_{50} = 9.4 \pm 0.5 \mu\text{M}$).

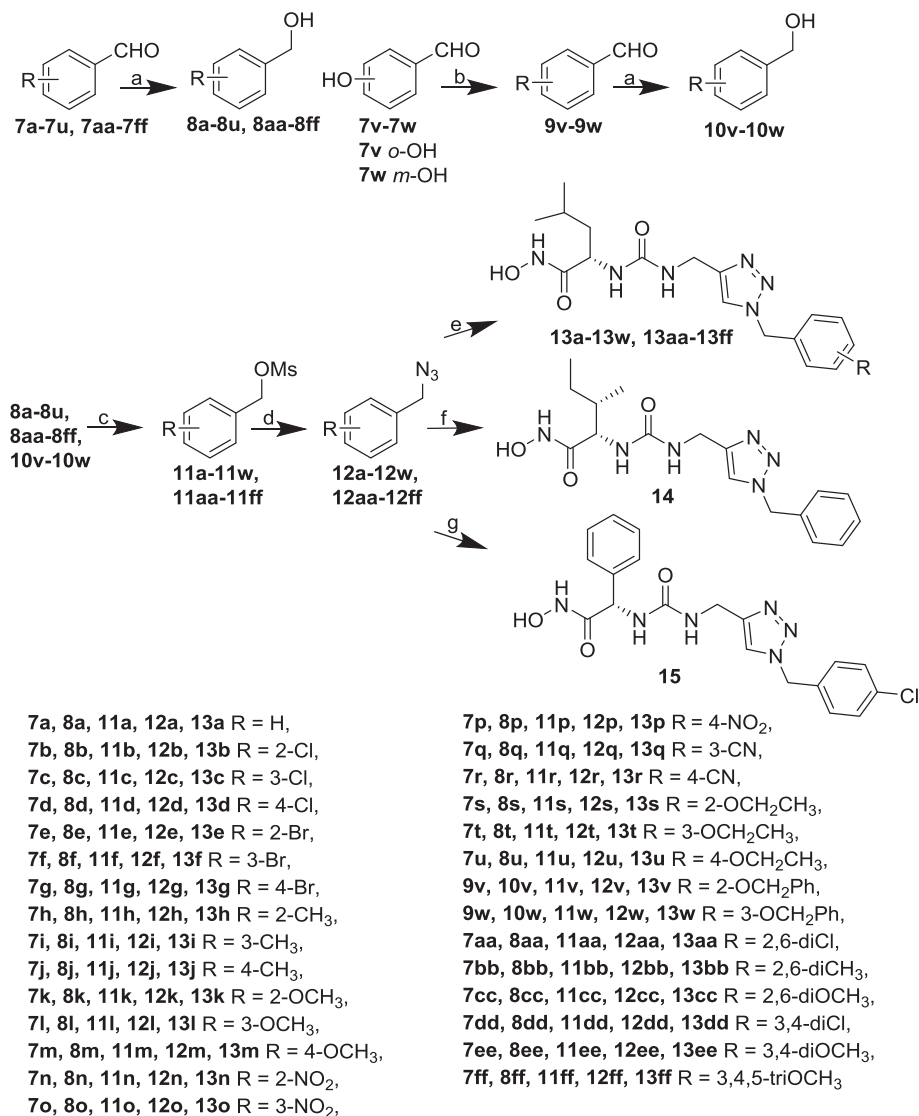
Furthermore, some compounds with potent enzyme inhibition activity were selected to evaluate their inhibitory capacities against human APN stemming from ES-2 and PLC/PRF/5 cell lines. The results in Table 2 show that compound **13v** was still the most potent compound with IC_{50} values over an order of magnitude lower than that of bestatin.

MTT assay was performed to evaluate the *in vitro* cytotoxicity of compounds **13v** and **13w**. The results listed in Table 3 show that both **13v** and **13w** presented better proliferation inhibition than bestatin against all the cell lines tested.

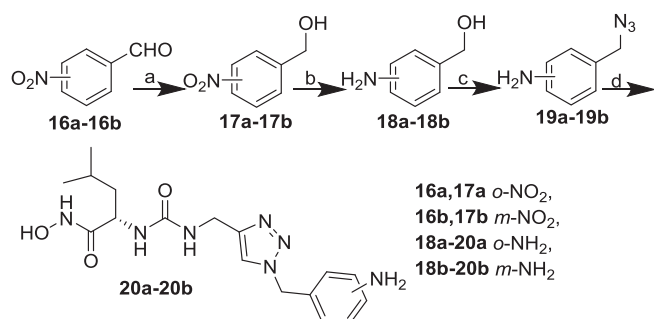
Compound **13v** was further progressed to human umbilical vein endothelial cells (HUVECs) tubular structure formation assay to evaluate its anti-angiogenesis activity. The results in Fig. 2 show that, compound **13v** could reduce the capillary tube formation in a dose-dependent manner. It was worth noting that $10 \mu\text{M}$ of **13v** presented similar anti-angiogenesis activity with $100 \mu\text{M}$ of bestatin.

It is considered that the rat aortic ring model could simulate the *in vivo* angiogenesis environment better than the HUVECs tube formation model. Our results in Fig. 3 show that compound **13v** could potentially reduce micro-vessel growth in a dose-dependent manner. Moreover, similar with the results in HUVECs tubular structure formation assay, $10 \mu\text{M}$ of compound **13v** demonstrated comparable micro-vessel growth inhibition relative to $100 \mu\text{M}$ of bestatin.

Based on the significant roles of APN in tumor metastasis^{5–7}, we used the mouse H22 hepatoma cell pulmonary metastasis model to evaluate the *in vivo* anti-metastasis activity of **13v**. The number of metastasis nodes on the surface of pulmonary lobes was counted to evaluate the anti-metastasis effect of tested compounds. As depicted in Fig. 4, the number of nodes in mice treated by **13v** (60 mg/kg , ip) was lower than that of mice treated by bestatin



Scheme 2. Reagents and conditions: (a) NaBH₄, MeOH, ice-bath, 1 h; (b) benzyl bromide, K₂CO₃, DMF, 80 °C, 5 h; (c) CH₃SO₂Cl, DCM, TEA, ice-bath, 12 h; (d) NaN₃, DMF, 25 °C, 12 h; (e) **6a** for **12a-12w** and **12aa-12ff**, CuSO₄·5H₂O, sodium ascorbate, DMSO/H₂O (4:1), 25 °C, 2 h; (f) **6b** for **12a**, CuSO₄·5H₂O, sodium ascorbate, DMSO/H₂O (4:1), 25 °C, 2 h; (g) **6c** for **12d**, CuSO₄·5H₂O, sodium ascorbate, DMSO/H₂O (4:1), 25 °C, 2 h.



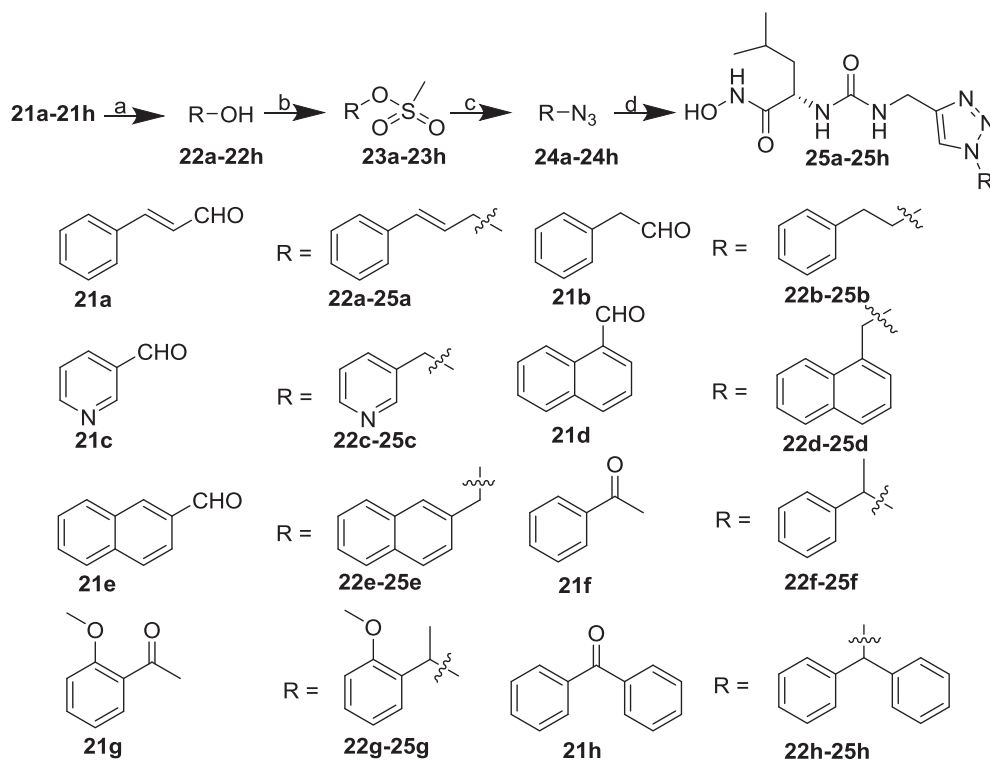
Scheme 3. Reagents and conditions: (a) NaBH₄, MeOH, ice-bath, 1 h; (b) Na₂S₂O₅, H₂O, 100 °C, 3 h; (c) Ph₃P, NaN₃, DMF, CCl₄, 100 °C, 12 h; (d) **6a**, CuSO₄·5H₂O, sodium ascorbate, DMSO/H₂O (4:1), 25 °C, 2 h.

(60 mg/kg, ip). The inhibitory rates of metastasis of **13v** and bestatin were 71% and 64%, respectively. There were no apparent loss of body weight and no evident toxic signs in liver and spleen in the group treated by **13v**.

In order to postulate its binding mode in APN, compound **13v** was docked into the active site of APN (PDB code: 2DQM) using Sybyl_X 1.3. As illustrated in Fig. 5A, the catalytic zinc ion of APN was chelated by the hydroxamate moiety of **13v**, and the S₁, S₁' and S₂' pockets of APN were occupied by the leucine residue, the two phenyl groups of **13v**, respectively. Moreover, the binding mode of **13a** (Fig. 5B) was also postulated and compared to that of **13v** (Fig. 5A). It could be found that both **13a** and **13v** chelated the zinc ion via the hydroxamate group and occupied the S₁ pocket via the leucine residue. Note that compound **13a** could only occupy the S₁' pocket with its single phenyl group, while compound **13v** could occupy the S₁' and S₂' pockets simultaneously. This might rationalize the better APN inhibitory activity of **13v**.

4. Conclusion

In summary, one novel series of triazole derivatives was designed, synthesized and evaluated as APNIs. In the enzymatic assay against APN, all leucine ureido-based compounds presented much better inhibitory activities than the positive control bestatin.



Scheme 4. Reagents and conditions: (a) NaBH₄, MeOH, ice-bath, 1 h; (b) CH₃SO₂Cl, DCM, TEA, ice-bath, 12 h; (c) NaN₃, DMF, 25 °C, 12 h; (d) **6a**, CuSO₄·5H₂O, sodium ascorbate, DMSO/H₂O (4:1), 25 °C, 2 h.

The best compound **13v** demonstrated more potent *in vitro* anti-angiogenesis activity than bestatin in both HUVECs tubular structure formation assay and rat aortic ring model. What's more, **13v** exhibited promising anti-metastasis effects in a mouse H22 pulmonary metastasis model, which deserve further research and development as anti-metastatic lead compound.

5. Experiment section

5.1. Chemistry: General procedures

All the materials were commercially available (Adamas-beta) and used without further purification otherwise noted. All reactions were monitored by thin-layer chromatography (TLC) on 0.25 mm silica gel plates (60 GF-254). UV light, ferric chloride and iodine vapor were used to visualize the spots. The products were purified by column chromatography or recrystallization. Melting points were determined on an electrothermal melting point apparatus without correction. ESI-MS were run on an API 4000 spectrometer. HRMS spectra were conducted by Shandong Analysis and Test Center. ¹H NMR and ¹³C NMR spectra were determined on a Bruker DRX spectrometer, and were described as δ in parts per million and J in Hertz, with TMS as an internal standard.

5.1.1. (S)-Methyl 4-methyl-2-(3-(prop-2-yn-1-yl)ureido)pentanoate (**5a**)

Compound **4a** (1.81 g, 10 mmol) was dissolved in a mixture solution of DCM (40 mL) and saturated NaHCO₃ (40 mL) followed by the addition of triphosgene (0.98 g, 3.3 mmol) gradually. The mixture was stirred in an ice-bath for 1.5 h. The organic layer was separated and dried over MgSO₄ for 15 min. After filtration, the residue was dropwise added into the solution of propargylamine (0.55 g, 10 mmol) and Et₃N (1.21 g, 12 mmol) in anhydrous DCM (100 mL) cooled in an ice-bath. After stirring at 25 °C for 12 h,

DCM was concentrated under vacuum. The residue was dissolved in EtOAc (100 mL) followed by washing with 10% HCl (3 × 100 mL), saturated NaHCO₃ (3 × 100 mL) and brine (3 × 100 mL), and drying over MgSO₄ overnight. EtOAc was evaporated and the obtained crude product was further purified by recrystallization from ethyl acetate/petroleum ether to give compound **5a** as a white solid (1.87 g, yield: 83%), mp: 102.9–104.2 °C. ¹H NMR (300 MHz, DMSO-*d*₆): δ 6.37 (d, J = 8.4 Hz, 1H), 6.25 (t, J = 5.7 Hz, 1H), 4.17 (q, J = 8.4 Hz, 1H), 3.78 (dd, J = 5.7 Hz, J = 2.4 Hz, 2H), 3.61 (s, 3H), 3.05 (t, J = 2.4 Hz, 1H), 1.68–1.54 (m, 1H), 1.47–1.42 (m, 2H), 0.89–0.84 (m, 6H); ESI-MS m/z 227.4 [M+H]⁺.

5.1.1.1. (2S,3R)-Methyl 3-methyl-2-(3-(prop-2-yn-1-yl)ureido)pentanoate (5b**).** White solid, yield: 81%, mp: 66.7–68.3 °C. ¹H NMR (400 MHz, DMSO-*d*₆): δ 6.36 (d, J = 12.0 Hz, 1H), 6.28 (t, J = 8.0 Hz, 1H), 4.12 (q, J = 12.0 Hz, 1H), 3.80 (dd, J = 8.0 Hz, J = 4.0 Hz, 2H), 3.62 (s, 3H), 3.07 (t, J = 4.0 Hz, 1H), 1.76–1.66 (m, 1H), 1.38–1.29 (m, 1H), 1.17–1.06 (m, 1H), 0.86–0.82 (m, 6H); ESI-MS m/z 227.4 [M+H]⁺.

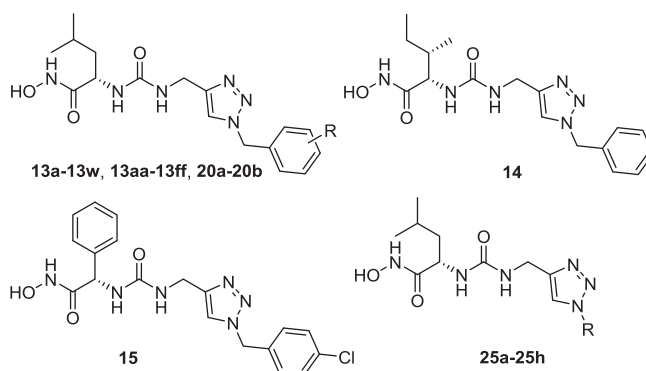
5.1.1.2. Methyl (S)-2-phenyl-2-(3-(prop-2-yn-1-yl)ureido)acetate (5c**).** White solid, yield: 75%, mp: 112.4–114.2 °C. ¹H NMR (400 MHz, DMSO-*d*₆): δ 7.41–7.33 (m, 5H), 6.95 (d, J = 8 Hz, 1H), 6.36 (t, J = 8 Hz, 1H), 5.28 (d, J = 8 Hz, 1H), 3.81 (dd, J = 8 Hz, 4 Hz, 2H), 3.62 (s, 3H), 3.08 (t, J = 4 Hz, 1H); ESI-MS m/z 247.4 [M+H]⁺.

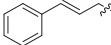
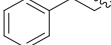
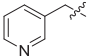
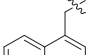
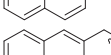
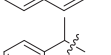
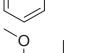
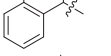
5.1.2. (S)-N-hydroxy-4-methyl-2-(3-(prop-2-yn-1-yl)ureido)pentanamide (**6a**)

The preparation of fresh methanol solution of potassium hydroxylamine.

Potassium hydroxide (28.00 g, 509 mmol) in anhydrous methanol (70 mL) was dropwise added into the anhydrous methanol (120 mL) solution of hydroxylamine hydrochloride (23.35 g, 343 mmol) cooled in an ice-bath. The mixture was stirred at 0 °C

Table 1
The structures and IC₅₀ values of target compounds against APN from porcine kidney.



Compd	R	IC ₅₀ (μM) ^a	Compd	R	IC ₅₀ (μM) ^a
13a	H	2.1 ± 0.2	13u	4-OCH ₂ CH ₃	1.5 ± 0.1
13b	2-Cl	0.67 ± 0.09	13v	2-OCH ₂ Ph	0.089 ± 0.007
13c	3-Cl	3.1 ± 0.2	13w	3-OCH ₂ Ph	0.24 ± 0.02
13d	4-Cl	6.9 ± 0.5	13aa	2,6-diCl	0.58 ± 0.06
13e	2-Br	0.88 ± 0.06	13bb	2,6-diCH ₃	0.39 ± 0.03
13f	3-Br	3.5 ± 0.3	13cc	2,6-diOCH ₃	0.47 ± 0.03
13g	4-Br	7.8 ± 0.5	13dd	3,4-diCl	5.5 ± 0.3
13h	2-CH ₃	0.76 ± 0.09	13ee	3,4-diOCH ₃	2.6 ± 0.2
13i	3-CH ₃	2.2 ± 0.1	13ff	3,4,5-triOCH ₃	1.4 ± 0.1
13j	4-CH ₃	3.6 ± 0.2	14	–	13.6 ± 2.1
13k	2-OCH ₃	0.65 ± 0.08	15	–	11.3 ± 1.7
13l	3-OCH ₃	0.91 ± 0.09	20a	2-NH ₂	0.68 ± 0.07
13m	4-OCH ₃	1.9 ± 0.1	20b	3-NH ₂	3.7 ± 0.3
13n	2-NO ₂	3.4 ± 0.1	25a		2.2 ± 0.1
13o	3-NO ₂	1.7 ± 0.3	25b		3.6 ± 0.3
13p	4-NO ₂	1.0 ± 0.1	25c		2.2 ± 0.1
13q	3-CN	7.8 ± 0.4	25d		1.4 ± 0.2
13r	4-CN	1.4 ± 0.2	25e		3.9 ± 0.3
13s	2-OCH ₂ CH ₃	0.44 ± 0.05	25f		1.9 ± 0.1
13t	3-OCH ₂ CH ₃	0.82 ± 0.05	25g		0.55 ± 0.04
Bestatin	–	9.4 ± 0.5	25h		2.3 ± 0.2

^a Assays were performed in triplicate; data are shown as mean \pm SD.

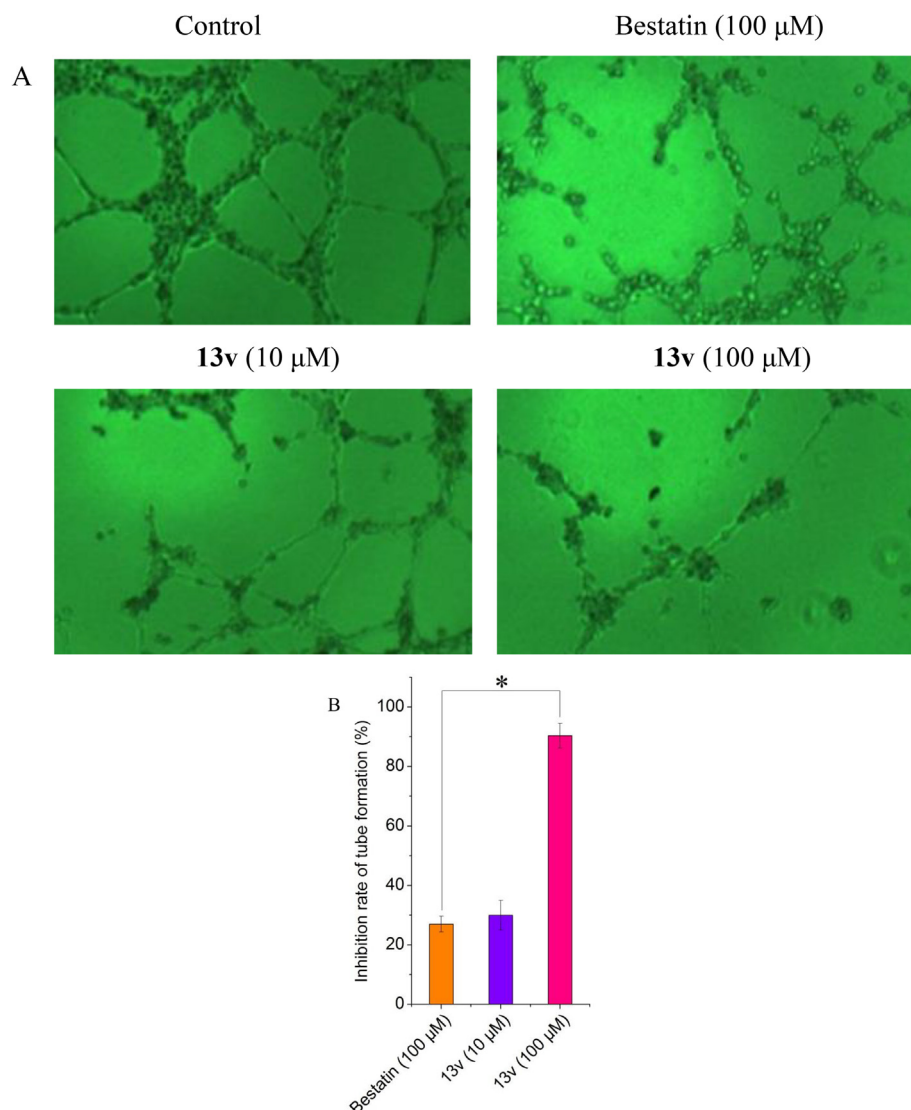
Table 2
The IC₅₀ values of selected compounds against APN on ES-2 and PLC/PRF/5 cell surfaces.

Compd	IC ₅₀ (μM) ^a		Compd	IC ₅₀ (μM) ^a	
	ES-2	PLC/PRF/5		ES-2	PLC/PRF/5
13h	6.9 ± 0.4	20.6 ± 1.0	13w	0.87 ± 0.1	4.9 ± 0.4
13k	6.5 ± 0.5	15.3 ± 1.2	25g	4.8 ± 0.3	12.3 ± 1.1
13s	2.1 ± 0.1	5.0 ± 0.3	Bestatin	35.5 ± 2.3	54.7 ± 3.5
13v	0.74 ± 0.08	1.3 ± 0.1			

^a Assays were performed in triplicate; data are shown as mean \pm SD.

Table 3The IC₅₀ values of selected compounds against proliferation of some tumor cell lines.

Compd	IC ₅₀ (μM) ^a							
	U937	HCT116	A549	ES-2	PLC	K562	MDA-MB-231	PC-3
13v	68.4 ± 6.3	81.2 ± 5.6	90.0 ± 2.9	104.6 ± 11.3	92.8 ± 5.6	85.0 ± 5.2	72.5 ± 3.6	119.1 ± 1.8
13w	70.3 ± 1.5	130.1 ± 12.8	128.0 ± 1.0	107.9 ± 12.5	112.2 ± 4.1	99.8 ± 13.1	72.6 ± 3.4	122.9 ± 7.9
Bestatin	>500	>500	>500	>500	>500	>500	>500	>500

^a Assays were performed in triplicate; data are shown as mean ± SD.**Fig. 2.** (A) Representative images of selected inhibitor **13v** on the formation of HUVECs capillary tube-like structure. (B) The inhibition rates of **13v** on the tubular structures formation of HUVECs. Data are expressed as the mean ± standard deviation from triplicate experiments. **P* < 0.05, **13v** (100 μM) vs bestatin (100 μM).

for 40 min and the precipitate was filtered out to provide a fresh methanol solution of potassium hydroxylamine.

Compound **5a** (2.26 g, 10 mmol) was dissolved in the solution above (20 mL) at 25 °C. The mixture was stirred at 25 °C for 0.5 h and then the methanol was evaporated. The residue was dissolved in water and then 10% HCl was added to adjust pH to 6. The mixture was extracted by EtOAc (3 × 100 mL). The organic layer was washed with saturated NaHCO₃ (3 × 100 mL) and brine (3 × 100 mL), and dried over MgSO₄. After evaporation of EtOAc under vacuum, DCM was added to the residue and then placed into refrigerator overnight. The formed precipitation was filtered off to give **6a**

as a white solid (1.20 g, yield: 53%), mp: 124.5–126.2 °C. ¹H NMR (600 MHz, DMSO-*d*₆): δ 10.68 (s, 1H), 8.80 (s, 1H), 6.24 (t, *J* = 5.7 Hz, 1H), 6.16 (d, *J* = 8.4 Hz, 1H), 4.05 (q, *J* = 8.4 Hz, 1H), 3.78 (dd, *J* = 5.7 Hz, *J* = 2.4 Hz, 2H), 3.05 (t, *J* = 2.4 Hz, 1H), 1.54–1.50 (m, 1H), 1.34–1.32 (m, 2H), 0.89–0.84 (m, 6H); ESI-MS *m/z* 226.3 [M–H][–].

5.1.2.1. (2S,3R)-N-hydroxy-3-methyl-2-(3-(prop-2-yn-1-yl)ureido)pentanamide (6b). White solid, yield: 51%, mp: 144.6–146.1 °C. ¹H NMR (400 MHz, DMSO-*d*₆): δ 10.64 (s, 1H), 8.82 (s, 1H), 6.34–6.28 (m, 1H), 6.22–6.14 (m, 1H), 4.01–3.83 (m, 1H), 3.80–3.77

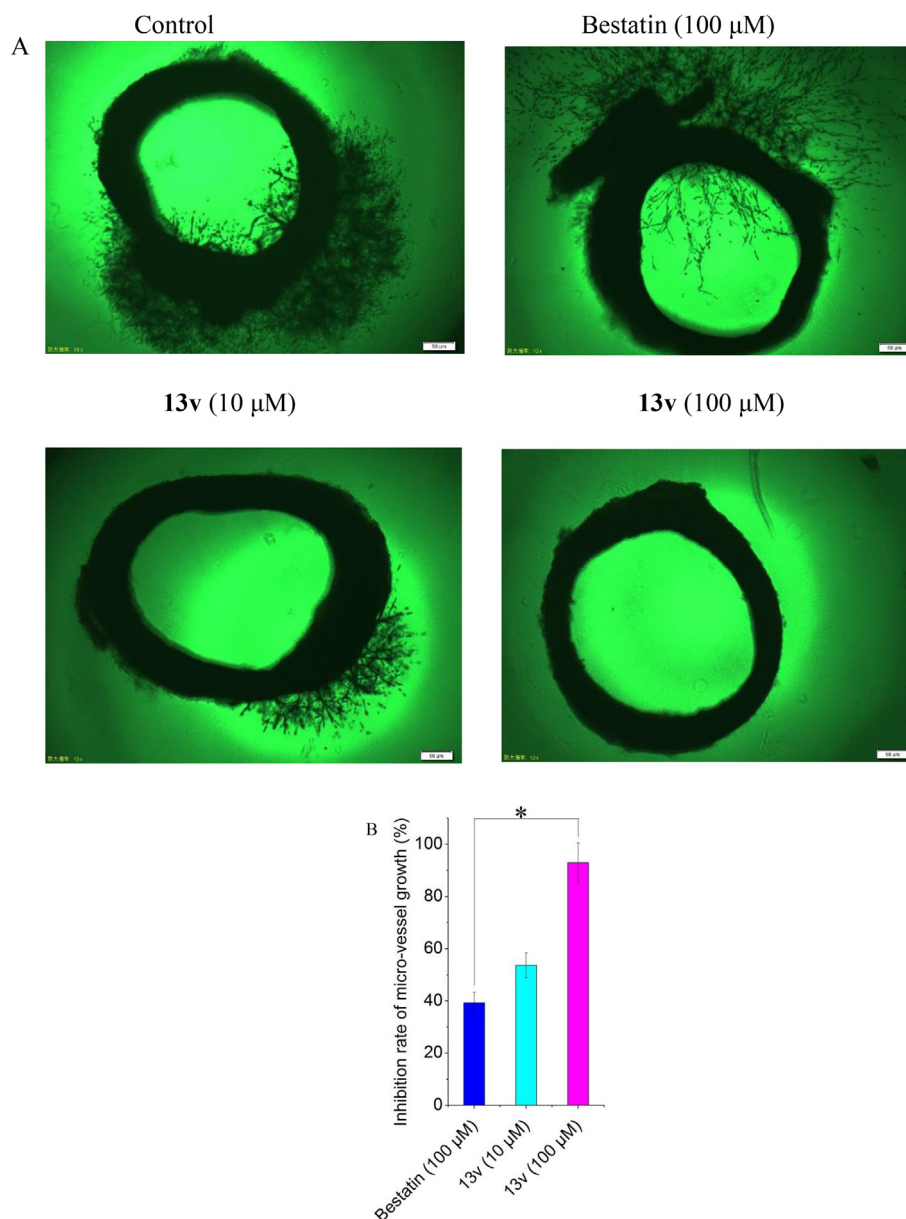


Fig. 3. (A) Representative images of selected inhibitor **13v** on the micro-vessels growth of the rat aortic ring. (B) The inhibition rates of **13v** on the micro-vessels growth. Data are expressed as the mean \pm standard deviation from triplicate experiments. * $P < 0.05$, **13v** (100 μ M) vs bestatin (100 μ M).

(m, 2H), 3.08–3.06 (m, 1H), 1.60–1.25 (m, 2H), 1.07–0.97 (m, 1H), 0.86–0.78 (m, 6H); ESI-MS m/z 228.4 $[M+H]^+$.

5.1.2.2. (S)-N-hydroxy-2-phenyl-2-(3-(prop-2-yn-1-yl)ureido)acetamide (6c). White solid, yield: 49%, mp: 136.4–138.2 °C. 1H NMR (400 MHz, DMSO- d_6): δ 11.00 (s, 1H), 8.95 (s, 1H), 7.37–7.30 (m, 5H), 6.96–6.90 (m, 1H), 6.37–6.34 (m, 1H), 5.29 (d, $J = 8$ Hz, 1H), 3.81 (dd, $J = 8$ Hz, 4 Hz, 2H), 3.08 (t, $J = 4$ Hz, 1H); ESI-MS m/z 248.3 $[M+H]^+$.

5.1.3. Phenylmethanol (8a)

To a solution of compound **7a** (1.06 g, 10 mmol) in methanol (10 mL) was added $NaBH_4$ (0.57 g, 15 mmol). After stirring for 1 h while cooled with an ice-water bath, methanol was evaporated and the residue was dissolved in EtOAc (100 mL). The organic layer was washed with water (3×100 mL) and brine (3×100 mL), and dried over $MgSO_4$ overnight. EtOAc was evaporated to give **8a** as colorless oil (2.01 g, yield: 94%). ESI-MS m/z 109.4 $[M+H]^+$. The

crude product was used directly in the next reaction without further purification.

Compounds **8b–8u**, **8aa–8ff**, **10v–10w**, **17a–17b** and **22a–22h** were prepared using the same procedure described above.

5.1.4. 2-(Benzyloxy)benzaldehyde (9v)

2-Hydroxybenzaldehyde **7v** (1.22 g, 10 mmol) and benzyl bromide (2.05 g, 12 mmol) were dissolved in DMF (20 mL). After addition of K_2CO_3 (2.07 g, 15 mmol), the mixture was heated at 80 °C for 5 h. The reaction was quenched by addition of ice-cold water (100 mL). Then the mixture was extracted by EtOAc (3×100 mL). The organic layer was washed by 10% HCl (3×100 mL), water (3×100 mL) and brine (3×100 mL), and dried over $MgSO_4$ overnight. EtOAc was evaporated to give compound **9v** as colorless oil (1.80 g, yield: 85%). ESI-MS m/z 213.4 $[M+H]^+$. The crude product was used directly in the next reaction without further purification.

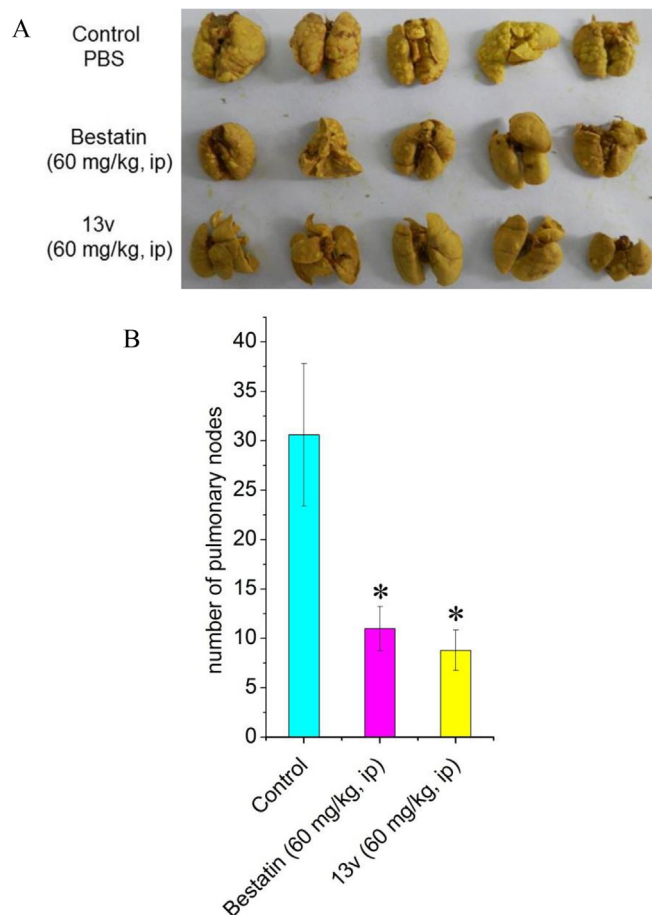


Fig. 4. Antitumor effect of **13v** on hepatoma cell H22 pulmonary metastasis model. (A) Picture of pulmonary lobes with metastatic nodes. (B) The number of metastatic pulmonary nodes. Data are expressed as mean \pm SD. * $P < 0.05$ versus control group.

Compound **9w** was prepared using the same procedure described above.

5.1.5. Benzyl methanesulfonate (**11a**)

To a solution of compound **8a** (1.08 g, 10 mmol) and Et_3N (1.52 g, 15 mmol) in anhydrous DCM (100 mL) was added dropwise methanesulfonyl chloride (1.36 g, 12 mmol) in anhydrous DCM (20 mL). The mixture was stirred for 12 h while being cooled with an ice-water bath. DCM was evaporated under vacuum. The residue was dissolved in EtOAc (100 mL) and washed with 10% HCl (3×100 mL), saturated NaHCO_3 (3×100 mL) and brine (3×100 mL), and then dried over MgSO_4 overnight. EtOAc was evaporated to give **11a** as yellow oil (1.77 g, yield: 95%). ESI-MS m/z 187.4 $[\text{M} + \text{H}]^+$. The crude product was used directly in the next reaction without further purification.

Compounds **11b–11w**, **11aa–11ff** and **23a–23h** were prepared using the same procedure described above.

5.1.6. (Azidomethyl)benzene (**12a**)

Compound **11a** (1.86 g, 10 mmol) was dissolved in DMF (10 mL) followed by the addition of NaN_3 (0.72 g, 11 mmol). The mixture was stirred at 25 °C for 12 h and then was quenched by being poured into ice-cold water. The mixture was extracted with EtOAc (3×100 mL). The organic layer was washed with water (3×100 mL) and brine (3×100 mL), and dried over MgSO_4 overnight. EtOAc was evaporated under vacuum to give **12a** as colorless oil (1.18 g, yield: 89%). ESI-MS m/z 134.4 $[\text{M} + \text{H}]^+$. The crude product was used directly in the next reaction without further purification.

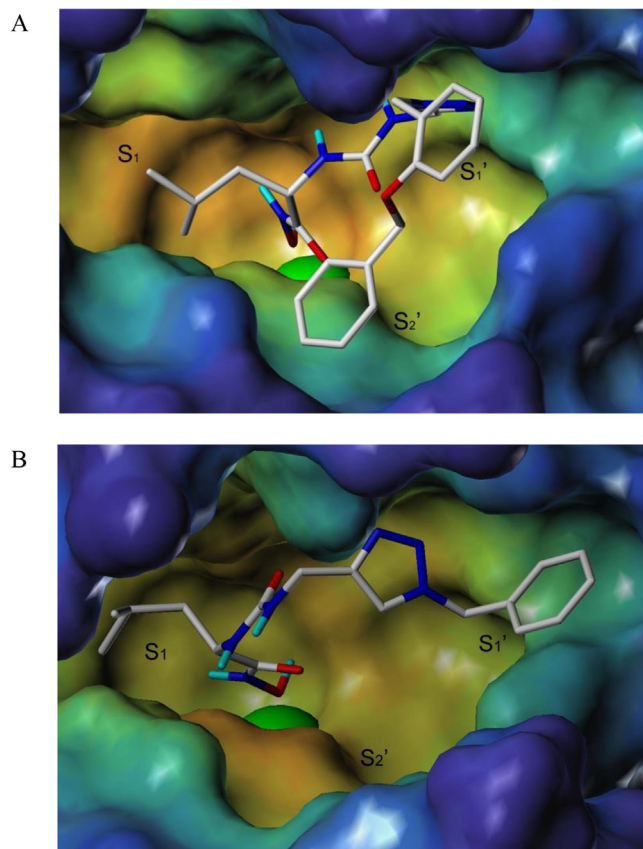


Fig. 5. The FlexX docking result of **13v** (A) and **13a** (B) in the active site of APN (PDB: 2DQM). The carbon atoms in white, nitrogen atoms in blue, oxygen atoms in red, hydrogen atoms in light blue and the green ball represents zinc ion. S_1 , S_1' and S_2' represent three hydrophobic pockets, respectively.

Compounds **12b–12w**, **12aa–12ff** and **24a–24h** were prepared using the same procedure described above.

5.1.7. (2-Aminophenyl)methanol (**18a**)

Compound **17a** (1.53 g, 10 mmol) was added into the solution of $\text{Na}_2\text{S} \cdot 9\text{H}_2\text{O}$ (21.60 g, 90 mmol) in water (100 mL). The mixture was heated at 100 °C for 3 h. After extraction by EtOAc, the organic layer was washed by water (3×100 mL) and brine (3×100 mL), and dried over MgSO_4 overnight. EtOAc was evaporated to give compound **18a** as a yellow solid (1.07 g, yield: 87%). ESI-MS m/z 124.5 $[\text{M} + \text{H}]^+$. The crude product was used directly in the next step without further purification.

Compound **18b** was prepared using the same procedure described above.

5.1.8. 2-(Azidomethyl)aniline (**19a**)

Compound **18a** (1.23 g, 10 mmol), triphenylphosphine (2.62 g, 10 mmol) and NaN_3 (0.78 g, 12 mmol) in DMF/ CCl_4 (16 mL/4 mL) was heated at 100 °C for 12 h. The mixture was poured into ice-cold water and extracted by Et_2O . The organic layer was washed with water (3×100 mL) and brine (3×100 mL), and dried over MgSO_4 overnight. Et_2O was concentrated to give the crude product. The product was purified by column chromatography (EtOAc/PE) to give **19a** as yellow oil (0.68 g, yield: 46%). ESI-MS m/z 149.5 $[\text{M} + \text{H}]^+$.

Compound **19b** was prepared using the same procedure described above.

5.1.9. (S)-2-(3-((1-Benzyl-1H-1,2,3-triazol-4-yl)methyl)ureido)-N-hydroxy-4-methylpentanamide (**13a**)

Compounds **6a** (0.45 g, 2 mmol) and **12a** (0.29 g, 2.2 mmol) were dissolved in DMSO (16 mL). Sodium ascorbate (59.4 mg, 0.3 mmol) in H₂O (2 mL) and CuSO₄·5H₂O (25 mg, 0.1 mmol) in H₂O (2 mL) were added into the above solution. The mixture was stirred at 25 °C for 2 h and poured into water (100 mL) and extracted by EtOAc (3 × 100 mL). The organic layer was washed by brine (3 × 100 mL) and dried over MgSO₄ overnight. EtOAc was evaporated to give colorless oil. The residue was dissolved in DCM and stirred for 2 h at 25 °C. The precipitate formed was filtered off to give 0.35 g of **13a** as a white solid. Yield: 48%, mp: 184.8–186.2 °C. ¹H NMR (600 MHz, DMSO *d*₆): δ 10.67 (s, 1H), 8.79 (s, 1H), 7.90 (s, 1H), 7.37 (t, *J* = 6.6 Hz, 2H), 7.32 (t, *J* = 6.6 Hz, 1H), 7.30 (d, *J* = 6.6 Hz, 2H), 6.36 (t, *J* = 6.0 Hz, 1H), 6.11 (d, *J* = 8.4 Hz, 1H), 5.56 (s, 2H), 4.21–4.20 (m, 2H), 4.06 (q, *J* = 8.4 Hz, 1H), 1.51–1.49 (m, 1H), 1.33–1.30 (m, 2H), 0.86–0.82 (m, 6H); ¹³C NMR (100 MHz, DMSO *d*₆): δ 169.9, 157.6, 146.6, 136.5, 129.1, 128.5, 128.3, 122.9, 53.1, 49.5, 42.9, 35.4, 24.6, 23.2, 22.6; HRMS (AP-ESI) *m/z* calcd for C₁₇H₂₅N₆O₃ [M+H]⁺ 361.1988, found 361.1992.

5.1.9.1. (S)-2-(3-((1-(2-Chlorobenzyl)-1H-1,2,3-triazol-4-yl)methyl)ureido)-N-hydroxy-4-methylpentanamide (**13b**). White solid, yield: 52%, mp: 154.6–156.3 °C. ¹H NMR (300 MHz, DMSO *d*₆): δ 10.66 (s, 1H), 8.79 (s, 1H), 7.87 (s, 1H), 7.54–7.50 (m, 1H), 7.43–7.29 (m, 2H), 7.23–7.19 (m, 1H), 6.38 (t, *J* = 5.7 Hz, 1H), 6.12 (d, *J* = 9.0 Hz, 1H), 5.67 (s, 2H), 4.22 (d, *J* = 5.7 Hz, 2H), 4.10–4.02 (m, 1H), 1.55–1.44 (m, 1H), 1.34–1.30 (m, 2H), 0.87–0.82 (m, 6H); ¹³C NMR (100 MHz, DMSO *d*₆): δ 169.8, 157.6, 146.5, 133.8, 133.0, 130.9, 130.6, 130.0, 128.1, 123.2, 50.9, 49.5, 42.9, 35.4, 24.6, 23.2, 22.6; HRMS (AP-ESI) *m/z* calcd for C₁₇H₂₄ClN₆O₃ [M+H]⁺ 395.1598, found 395.1590.

5.1.9.2. (S)-2-(3-((1-(3-Chlorobenzyl)-1H-1,2,3-triazol-4-yl)methyl)ureido)-N-hydroxy-4-methylpentanamide (**13c**). White solid, yield: 55%, mp: 186.8–188.5 °C. ¹H NMR (300 MHz, DMSO *d*₆): δ 10.67 (s, 1H), 8.80 (s, 1H), 7.95 (s, 1H), 7.41–7.40 (m, 3H), 7.28–7.24 (m, 1H), 6.39 (t, *J* = 5.4 Hz, 1H), 6.13 (d, *J* = 8.7 Hz, 1H), 5.59 (s, 2H), 4.22 (d, *J* = 5.4 Hz, 2H), 4.11–4.03 (m, 1H), 1.55–1.44 (m, 1H), 1.35–1.30 (m, 2H), 0.87–0.82 (m, 6H); ¹³C NMR (100 MHz, DMSO *d*₆): δ 169.8, 157.6, 146.7, 138.9, 133.7, 131.1, 128.5, 128.2, 127.1, 123.1, 52.3, 49.6, 42.9, 35.4, 24.6, 23.2, 22.6; HRMS (AP-ESI) *m/z* calcd for C₁₇H₂₄ClN₆O₃ [M+H]⁺ 395.1598, found 395.1601.

5.1.9.3. (S)-2-(3-((1-(4-Chlorobenzyl)-1H-1,2,3-triazol-4-yl)methyl)ureido)-N-hydroxy-4-methylpentanamide (**13d**). White solid, yield: 51%, mp: 180.8–182.5 °C. ¹H NMR (300 MHz, DMSO *d*₆): δ 10.66 (s, 1H), 8.78 (s, 1H), 7.91 (s, 1H), 7.44 (d, *J* = 8.4 Hz, 2H), 7.32 (d, *J* = 8.4 Hz, 2H), 6.36 (t, *J* = 5.4 Hz, 1H), 6.11 (d, *J* = 8.7 Hz, 1H), 5.57 (s, 2H), 4.28 (d, *J* = 5.4 Hz, 2H), 4.09–4.01 (m, 1H), 1.57–1.44 (m, 1H), 1.34–1.30 (m, 2H), 0.87–0.82 (m, 6H); ¹³C NMR (100 MHz, DMSO *d*₆): δ 169.8, 157.6, 146.7, 135.5, 133.2, 130.3, 129.1, 123.0, 52.3, 49.5, 42.9, 35.4, 24.6, 23.2, 22.6; HRMS (AP-ESI) *m/z* calcd for C₁₇H₂₄ClN₆O₃ [M+H]⁺ 395.1598, found 395.1607.

5.1.9.4. (S)-2-(3-((1-(2-Bromobenzyl)-1H-1,2,3-triazol-4-yl)methyl)ureido)-N-hydroxy-4-methylpentanamide (**13e**). White solid, yield: 47%, mp: 144.8–146.2 °C. ¹H NMR (300 MHz, DMSO *d*₆): δ 10.66 (s, 1H), 8.78 (s, 1H), 7.87 (s, 1H), 7.69 (dd, *J* = 7.8 Hz, *J* = 1.2 Hz, 1H), 7.41 (td, *J* = 7.8 Hz, *J* = 1.2 Hz, 1H), 7.31 (td, *J* = 7.8 Hz, *J* = 1.8 Hz, 1H), 7.14 (dd, *J* = 7.8 Hz, *J* = 1.8 Hz, 1H), 6.38 (t, *J* = 5.7 Hz, 1H), 6.12 (d, *J* = 9.0 Hz, 1H), 5.65 (s, 2H), 4.23 (d, *J* = 5.7 Hz, 2H), 4.10–4.02 (m, 1H), 1.57–1.44 (m, 1H), 1.34–1.29 (m, 2H), 0.87–0.82 (m, 6H); ¹³C NMR (100 MHz, DMSO *d*₆): δ 169.8, 157.6, 146.5, 135.4, 133.3, 130.8, 130.8, 128.7, 123.3, 53.2, 49.5, 42.9, 35.4,

24.6, 23.2, 22.6; HRMS (AP-ESI) *m/z* calcd for C₁₇H₂₄BrN₆O₃ [M+H]⁺ 439.1093, found 439.1093.

5.1.9.5. (S)-2-(3-((1-(3-Bromobenzyl)-1H-1,2,3-triazol-4-yl)methyl)ureido)-N-hydroxy-4-methylpentanamide (**13f**). White solid, yield: 49%, mp: 168.9–170.4 °C. ¹H NMR (300 MHz, DMSO *d*₆): δ 10.66 (s, 1H), 8.79 (s, 1H), 7.95 (s, 1H), 7.55–7.53 (m, 1H), 7.40–7.28 (m, 3H), 6.38 (t, *J* = 5.7 Hz, 1H), 6.12 (d, *J* = 8.7 Hz, 1H), 5.58 (s, 2H), 4.22 (d, *J* = 5.7 Hz, 2H), 4.10–4.02 (m, 1H), 1.55–1.44 (m, 1H), 1.34–1.29 (m, 2H), 0.87–0.82 (m, 6H); ¹³C NMR (100 MHz, DMSO *d*₆): δ 169.8, 157.6, 146.2, 139.2, 129.1, 128.6, 128.4, 128.4, 123.0, 67.0, 49.5, 42.8, 35.4, 24.6, 23.2, 22.5; HRMS (AP-ESI) *m/z* calcd for C₁₇H₂₄BrN₆O₃ [M+H]⁺ 439.1093, found 439.1090.

5.1.9.6. (S)-2-(3-((1-(4-Bromobenzyl)-1H-1,2,3-triazol-4-yl)methyl)ureido)-N-hydroxy-4-methylpentanamide (**13g**). White solid, yield: 46%, mp: 178.8–180.3 °C. ¹H NMR (300 MHz, DMSO *d*₆): δ 10.66 (s, 1H), 8.79 (s, 1H), 7.91 (s, 1H), 7.57 (d, *J* = 8.4 Hz, 2H), 7.26 (d, *J* = 8.4 Hz, 2H), 6.37 (t, *J* = 5.7 Hz, 1H), 6.12 (d, *J* = 9.0 Hz, 1H), 5.55 (s, 2H), 4.21 (d, *J* = 5.7 Hz, 2H), 4.10–4.02 (m, 1H), 1.57–1.44 (m, 1H), 1.34–1.29 (m, 2H), 0.87–0.82 (m, 6H); ¹³C NMR (100 MHz, DMSO *d*₆): δ 169.8, 157.6, 146.7, 136.0, 132.1, 130.6, 123.0, 121.8, 52.4, 49.5, 42.9, 35.4, 24.6, 23.2, 22.6; HRMS (AP-ESI) *m/z* calcd for C₁₇H₂₄BrN₆O₃ [M+H]⁺ 439.1093, found 439.1091.

5.1.9.7. (S)-N-hydroxy-4-methyl-2-(3-((1-(2-methylbenzyl)-1H-1,2,3-triazol-4-yl)methyl)ureido)pentanamide (**13h**). White solid, yield: 48%, mp: 166.6–168.3 °C. ¹H NMR (300 MHz, DMSO *d*₆): δ 10.66 (s, 1H), 8.78 (s, 1H), 7.78 (s, 1H), 7.27–7.16 (m, 3H), 7.09–7.06 (m, 1H), 6.36 (t, *J* = 5.7 Hz, 1H), 6.11 (d, *J* = 8.7 Hz, 1H), 5.57 (s, 2H), 4.21 (d, *J* = 5.7 Hz, 2H), 4.09–4.01 (m, 1H), 2.30 (s, 3H), 1.57–1.42 (m, 1H), 1.34–1.29 (m, 2H), 0.87–0.82 (m, 6H); ¹³C NMR (100 MHz, DMSO *d*₆): δ 169.8, 157.6, 146.5, 136.7, 134.6, 130.8, 129.1, 128.7, 126.6, 122.9, 51.3, 49.5, 42.9, 35.4, 24.6, 23.2, 22.6, 19.0; HRMS (AP-ESI) *m/z* calcd for C₁₈H₂₇N₆O₃ [M+H]⁺ 375.2145, found 375.2150.

5.1.9.8. (S)-N-hydroxy-4-methyl-2-(3-((1-(3-methylbenzyl)-1H-1,2,3-triazol-4-yl)methyl)ureido)pentanamide (**13i**). White solid, yield: 55%, mp: 184.8–186.3 °C. ¹H NMR (300 MHz, DMSO *d*₆): δ 10.66 (s, 1H), 8.79 (s, 1H), 7.88 (s, 1H), 7.28–7.23 (m, 1H), 7.15–7.08 (m, 3H), 6.36 (t, *J* = 5.7 Hz, 1H), 6.11 (d, *J* = 8.7 Hz, 1H), 5.51 (s, 2H), 4.21 (d, *J* = 5.7 Hz, 2H), 4.10–4.02 (m, 1H), 2.28 (s, 3H), 1.57–1.44 (m, 1H), 1.34–1.29 (m, 2H), 0.87–0.82 (m, 6H); ¹³C NMR (100 MHz, DMSO *d*₆): δ 169.8, 157.6, 146.5, 138.4, 136.4, 129.2, 129.1, 129.0, 125.5, 122.8, 53.1, 49.5, 42.9, 35.4, 24.6, 23.2, 22.6, 21.3; HRMS (AP-ESI) *m/z* calcd for C₁₈H₂₇N₆O₃ [M+H]⁺ 375.2145, found 375.2151.

5.1.9.9. (S)-N-hydroxy-4-methyl-2-(3-((1-(4-methylbenzyl)-1H-1,2,3-triazol-4-yl)methyl)ureido)pentanamide (**13j**). White solid, yield: 57%, mp: 180.4–182.2 °C. ¹H NMR (300 MHz, DMSO *d*₆): δ 10.66 (s, 1H), 8.79 (s, 1H), 7.85 (s, 1H), 7.21 (d, *J* = 8.1 Hz, 2H), 7.17 (d, *J* = 8.1 Hz, 2H), 6.35 (t, *J* = 5.7 Hz, 1H), 6.10 (d, *J* = 9.0 Hz, 1H), 5.50 (s, 2H), 4.20 (d, *J* = 5.7 Hz, 2H), 4.09–4.01 (m, 1H), 2.28 (s, 3H), 1.57–1.44 (m, 1H), 1.34–1.29 (m, 2H), 0.87–0.82 (m, 6H); ¹³C NMR (100 MHz, DMSO *d*₆): δ 169.8, 157.6, 146.5, 137.9, 133.5, 129.7, 128.4, 122.7, 53.0, 49.5, 42.9, 35.4, 24.6, 23.2, 22.6, 21.1; HRMS (AP-ESI) *m/z* calcd for C₁₈H₂₇N₆O₃ [M+H]⁺ 375.2145, found 375.2137.

5.1.9.10. (S)-N-hydroxy-2-(3-((1-(2-methoxybenzyl)-1H-1,2,3-triazol-4-yl)methyl)ureido)-4-methylpentanamide (**13k**). White solid, yield: 53%, mp: 160.8–162.3 °C. ¹H NMR (300 MHz, DMSO *d*₆): δ 10.67 (s, 1H), 8.79 (s, 1H), 7.75 (s, 1H), 7.37–7.32 (m, 1H), 7.11–7.04 (m, 2H), 6.96–6.91 (m, 1H), 6.36 (t, *J* = 5.7 Hz, 1H), 6.11 (d, *J*

= 8.7 Hz, 1H), 5.49 (s, 2H), 4.20 (d, J = 5.7 Hz, 2H), 4.10–4.02 (m, 1H), 3.82 (s, 3H), 1.57–1.44 (m, 1H), 1.34–1.29 (m, 2H), 0.87–0.82 (m, 6H); ^{13}C NMR (100 MHz, DMSO d_6): δ 169.8, 157.6, 157.2, 146.2, 130.4, 130.0, 124.0, 122.9, 120.9, 111.7, 56.0, 49.5, 48.6, 42.9, 35.4, 24.6, 23.2, 22.6; HRMS (AP-ESI) m/z calcd for $\text{C}_{18}\text{H}_{27}\text{N}_6\text{O}_4$ $[\text{M}+\text{H}]^+$ 391.2094, found 391.2091.

5.1.9.11. (*S*)-*N*-hydroxy-2-(3-((1-(3-methoxybenzyl)-1*H*-1,2,3-triazol-4-yl)methyl)ureido)-4-methylpentanamide (**13l**). White solid, yield: 51%, mp: 174.5–176.2 °C. ^1H NMR (300 MHz, DMSO d_6): δ 10.67 (s, 1H), 8.79 (s, 1H), 7.90 (s, 1H), 7.31–7.25 (m, 1H), 6.91–6.83 (m, 3H), 6.37 (t, J = 5.7 Hz, 1H), 6.11 (d, J = 9.0 Hz, 1H), 5.52 (s, 2H), 4.21 (d, J = 5.7 Hz, 2H), 4.10–4.02 (m, 1H), 3.74 (s, 3H), 1.57–1.44 (m, 1H), 1.34–1.29 (m, 2H), 0.87–0.82 (m, 6H); ^{13}C NMR (100 MHz, DMSO d_6): δ 169.8, 159.8, 157.6, 146.5, 137.9, 130.3, 123.0, 120.4, 114.2, 113.8, 55.5, 53.0, 49.5, 42.8, 35.3, 24.6, 23.1, 22.5; HRMS (AP-ESI) m/z calcd for $\text{C}_{18}\text{H}_{27}\text{N}_6\text{O}_4$ $[\text{M}+\text{H}]^+$ 391.2094, found 391.2084.

5.1.9.12. (*S*)-*N*-hydroxy-2-(3-((1-(4-methoxybenzyl)-1*H*-1,2,3-triazol-4-yl)methyl)ureido)-4-methylpentanamide (**13m**). White solid, yield: 54%, mp: 164.8–166.3 °C. ^1H NMR (300 MHz, DMSO d_6): δ 10.66 (s, 1H), 8.79 (s, 1H), 7.83 (s, 1H), 7.28 (d, J = 8.7 Hz, 2H), 6.92 (d, J = 8.7 Hz, 2H), 6.35 (t, J = 5.7 Hz, 1H), 6.11 (d, J = 8.7 Hz, 1H), 5.47 (s, 2H), 4.19 (d, J = 5.7 Hz, 2H), 4.09–4.01 (m, 1H), 3.73 (s, 3H), 1.55–1.44 (m, 1H), 1.34–1.29 (m, 2H), 0.87–0.82 (m, 6H); ^{13}C NMR (100 MHz, DMSO d_6): δ 169.8, 159.5, 157.5, 146.5, 130.0, 128.4, 122.5, 114.5, 55.6, 52.7, 49.5, 42.9, 35.4, 24.6, 23.2, 22.6; HRMS (AP-ESI) m/z calcd for $\text{C}_{18}\text{H}_{27}\text{N}_6\text{O}_4$ $[\text{M}+\text{H}]^+$ 391.2094, found 391.2097.

5.1.9.13. (*S*)-*N*-hydroxy-4-methyl-2-(3-((1-(2-nitrobenzyl)-1*H*-1,2,3-triazol-4-yl)methyl)ureido)pentanamide (**13n**). Yellow solid, yield: 58%, mp: 168.7–170.5 °C. ^1H NMR (300 MHz, DMSO d_6): δ 10.64 (s, 1H), 8.80 (s, 1H), 8.14 (dd, J = 7.5 Hz, J = 1.2 Hz, 1H), 7.93 (s, 1H), 7.74 (td, J = 7.5 Hz, J = 1.2 Hz, 1H), 7.63 (td, J = 7.5 Hz, J = 1.2 Hz, 1H), 7.01 (d, J = 7.5 Hz, 1H), 6.41 (t, J = 5.7 Hz, 1H), 6.15 (d, J = 8.7 Hz, 1H), 5.94 (s, 2H), 4.25 (d, J = 5.7 Hz, 2H), 4.10–4.02 (m, 1H), 1.55–1.44 (m, 1H), 1.34–1.30 (m, 2H), 0.87–0.82 (m, 6H); ^{13}C NMR (100 MHz, DMSO d_6): δ 169.8, 157.6, 148.0, 146.7, 134.7, 131.4, 130.4, 130.0, 125.4, 123.7, 50.2, 49.5, 42.9, 35.4, 24.6, 23.2, 22.6; HRMS (AP-ESI) m/z calcd for $\text{C}_{17}\text{H}_{24}\text{N}_7\text{O}_5$ $[\text{M}+\text{H}]^+$ 406.1839, found 406.1845.

5.1.9.14. (*S*)-*N*-hydroxy-4-methyl-2-(3-((1-(3-nitrobenzyl)-1*H*-1,2,3-triazol-4-yl)methyl)ureido)pentanamide (**13o**). Yellow solid, yield: 57%, mp: 186.8–188.3 °C. ^1H NMR (300 MHz, DMSO d_6): δ 10.68 (s, 1H), 8.80 (s, 1H), 8.23–8.19 (m, 2H), 8.02 (s, 1H), 7.76 (d, J = 7.8 Hz, 1H), 7.69 (t, J = 7.8 Hz, 1H), 6.40 (t, J = 5.7 Hz, 1H), 6.13 (d, J = 8.7 Hz, 1H), 5.75 (s, 2H), 4.23 (d, J = 5.7 Hz, 2H), 4.10–4.02 (m, 1H), 1.57–1.44 (m, 1H), 1.34–1.30 (m, 2H), 0.87–0.82 (m, 6H); ^{13}C NMR (100 MHz, DMSO d_6): δ 169.8, 157.6, 148.3, 146.8, 138.7, 135.1, 130.8, 123.5, 123.3, 123.2, 52.1, 49.5, 42.8, 35.3, 24.6, 23.1, 22.6; HRMS (AP-ESI) m/z calcd for $\text{C}_{17}\text{H}_{24}\text{N}_7\text{O}_5$ $[\text{M}+\text{H}]^+$ 406.1839, found 406.1845.

5.1.9.15. (*S*)-*N*-hydroxy-4-methyl-2-(3-((1-(4-nitrobenzyl)-1*H*-1,2,3-triazol-4-yl)methyl)ureido)pentanamide (**13p**). Yellow solid, yield: 58%, mp: 176.9–178.4 °C. ^1H NMR (300 MHz, DMSO d_6): δ 10.68 (s, 1H), 8.80 (s, 1H), 8.24 (d, J = 8.7 Hz, 2H), 8.00 (s, 1H), 7.52 (d, J = 8.7 Hz, 2H), 6.40 (t, J = 5.1 Hz, 1H), 6.14 (d, J = 8.7 Hz, 1H), 5.76 (s, 2H), 4.24 (d, J = 5.1 Hz, 2H), 4.10–4.02 (m, 1H), 1.55–1.44 (m, 1H), 1.35–1.30 (m, 2H), 0.87–0.82 (m, 6H); ^{13}C NMR (100 MHz, DMSO d_6): δ 169.8, 157.6, 147.6, 146.8, 144.0, 129.4, 124.3, 123.4, 52.2, 49.5, 42.8, 35.3, 24.6, 23.1, 22.6; HRMS (AP-ESI) m/z calcd for $\text{C}_{17}\text{H}_{24}\text{N}_7\text{O}_5$ $[\text{M}+\text{H}]^+$ 406.1839, found 406.1836.

5.1.9.16. (*S*)-2-(3-((1-(3-Cyanobenzyl)-1*H*-1,2,3-triazol-4-yl)methyl)ureido)-*N*-hydroxy-4-methylpentanamide (**13q**). White solid, yield: 52%, mp: 180.7–182.3 °C. ^1H NMR (300 MHz, DMSO d_6): δ 10.68 (s, 1H), 8.83 (s, 1H), 7.99 (s, 1H), 7.87–7.81 (m, 2H), 7.65–7.57 (m, 2H), 6.39 (t, J = 5.4 Hz, 1H), 6.13 (d, J = 9.0 Hz, 1H), 5.65 (s, 2H), 4.22 (d, J = 5.4 Hz, 2H), 4.10–4.02 (m, 1H), 1.55–1.44 (m, 1H), 1.35–1.30 (m, 2H), 0.87–0.82 (m, 6H); ^{13}C NMR (100 MHz, DMSO d_6): δ 169.8, 157.6, 146.7, 138.1, 133.4, 132.4, 132.0, 130.5, 123.2, 118.9, 112.1, 52.2, 49.5, 42.8, 35.3, 24.6, 23.2, 22.5; HRMS (AP-ESI) m/z calcd for $\text{C}_{18}\text{H}_{24}\text{N}_7\text{O}_3$ $[\text{M}+\text{H}]^+$ 386.1941, found 386.1937.

5.1.9.17. (*S*)-2-(3-((1-(4-Cyanobenzyl)-1*H*-1,2,3-triazol-4-yl)methyl)ureido)-*N*-hydroxy-4-methylpentanamide (**13r**). White solid, yield: 48%, mp: 172.3–174.1 °C. ^1H NMR (300 MHz, DMSO d_6): δ 10.68 (s, 1H), 8.81 (s, 1H), 7.97 (s, 1H), 7.86 (d, J = 8.1 Hz, 2H), 7.44 (d, J = 8.1 Hz, 2H), 6.39 (t, J = 5.7 Hz, 1H), 6.13 (d, J = 9.0 Hz, 1H), 5.70 (s, 2H), 4.28 (d, J = 5.7 Hz, 2H), 4.10–4.02 (m, 1H), 1.57–1.44 (m, 1H), 1.34–1.30 (m, 2H), 0.87–0.82 (m, 6H); ^{13}C NMR (100 MHz, DMSO d_6): δ 169.8, 157.6, 146.7, 142.0, 133.1, 129.1, 123.4, 119.0, 111.3, 52.5, 49.5, 42.8, 35.3, 24.6, 23.2, 22.6; HRMS (AP-ESI) m/z calcd for $\text{C}_{18}\text{H}_{24}\text{N}_7\text{O}_3$ $[\text{M}+\text{H}]^+$ 386.1941, found 386.1944.

5.1.9.18. (*S*)-2-(3-((1-(2-Ethoxybenzyl)-1*H*-1,2,3-triazol-4-yl)methyl)ureido)-*N*-hydroxy-4-methylpentanamide (**13s**). White solid, yield: 58%, mp: 154.5–156.1 °C. ^1H NMR (300 MHz, DMSO d_6): δ 10.66 (s, 1H), 8.77 (s, 1H), 7.74 (s, 1H), 7.32 (td, J = 7.5 Hz, J = 1.5 Hz, 1H), 7.13 (dd, J = 7.5 Hz, J = 1.5 Hz, 1H), 7.03 (d, J = 7.5 Hz, 1H), 6.92 (td, J = 7.5 Hz, J = 1.5 Hz, 1H), 6.36 (t, J = 5.4 Hz, 1H), 6.11 (d, J = 8.7 Hz, 1H), 5.48 (s, 2H), 4.20 (d, J = 5.4 Hz, 2H), 4.09–4.02 (m, 3H), 1.55–1.42 (m, 1H), 1.35–1.29 (m, 5H), 0.87–0.82 (m, 6H); ^{13}C NMR (100 MHz, DMSO d_6): δ 169.8, 157.6, 156.6, 146.2, 130.3, 130.2, 124.2, 123.0, 120.8, 112.5, 64.0, 49.5, 48.8, 42.9, 35.4, 24.6, 23.2, 22.6, 15.0; HRMS (AP-ESI) m/z calcd for $\text{C}_{19}\text{H}_{29}\text{N}_6\text{O}_4$ $[\text{M}+\text{H}]^+$ 405.2250, found 405.2258.

5.1.9.19. (*S*)-2-(3-((1-(3-Ethoxybenzyl)-1*H*-1,2,3-triazol-4-yl)methyl)ureido)-*N*-hydroxy-4-methylpentanamide (**13t**). White solid, yield: 55%, mp: 156.8–158.3 °C. ^1H NMR (400 MHz, DMSO d_6): δ 10.66 (s, 1H), 8.78 (s, 1H), 7.89 (s, 1H), 7.26 (t, J = 8.0 Hz, J = 1.5 Hz, 1H), 6.89–6.82 (m, 3H), 6.37 (t, J = 8.0 Hz, 1H), 6.11 (d, J = 8.0 Hz, 1H), 5.51 (s, 2H), 4.21 (d, J = 8.0 Hz, 2H), 4.09–3.97 (m, 3H), 1.54–1.46 (m, 1H), 1.34–1.29 (m, 5H), 0.87–0.82 (m, 6H); ^{13}C NMR (100 MHz, DMSO d_6): δ 169.8, 159.1, 157.6, 146.5, 137.9, 130.3, 122.9, 120.3, 114.7, 114.2, 63.4, 53.1, 49.5, 42.9, 35.4, 24.6, 23.2, 22.6, 15.0; HRMS (AP-ESI) m/z calcd for $\text{C}_{19}\text{H}_{29}\text{N}_6\text{O}_4$ $[\text{M}+\text{H}]^+$ 405.2250, found 405.2258.

5.1.9.20. (*S*)-2-(3-((1-(4-Ethoxybenzyl)-1*H*-1,2,3-triazol-4-yl)methyl)ureido)-*N*-hydroxy-4-methylpentanamide (**13u**). White solid, yield: 51%, mp: 164.6–166.2 °C. ^1H NMR (400 MHz, DMSO d_6): δ 10.65 (s, 1H), 8.78 (s, 1H), 7.83 (s, 1H), 7.26 (d, J = 8.0 Hz, 2H), 6.90 (d, J = 8.0 Hz, 2H), 6.35 (t, J = 8.0 Hz, 1H), 6.09 (d, J = 8.0 Hz, 1H), 5.46 (s, 2H), 4.20 (d, J = 8.0 Hz, 2H), 4.08–3.97 (m, 3H), 1.53–1.47 (m, 1H), 1.33–1.28 (m, 5H), 0.86–0.82 (m, 6H); ^{13}C NMR (100 MHz, DMSO d_6): δ 169.8, 158.8, 157.6, 146.5, 130.0, 128.3, 122.5, 115.0, 63.5, 52.7, 49.5, 42.9, 35.4, 24.6, 23.2, 22.6, 15.0; HRMS (AP-ESI) m/z calcd for $\text{C}_{19}\text{H}_{29}\text{N}_6\text{O}_4$ $[\text{M}+\text{H}]^+$ 405.2250, found 405.2268.

5.1.9.21. (*S*)-2-(3-((1-(2-(Benzyloxy)benzyl)-1*H*-1,2,3-triazol-4-yl)methyl)ureido)-*N*-hydroxy-4-methylpentanamide (**13v**). White solid, yield: 47%, mp: 124.8–126.5 °C. ^1H NMR (300 MHz, DMSO d_6): δ 10.66 (s, 1H), 8.78 (s, 1H), 7.72 (s, 1H), 7.48–7.29 (m, 6H), 7.13 (d, J = 7.8 Hz, 2H), 6.94 (t, J = 7.8 Hz, 1H), 6.36 (t, J = 5.7 Hz, 1H), 6.12 (d, J = 9.0 Hz, 1H), 5.55 (s, 2H), 5.17 (s, 2H), 4.21 (d, J = 5.7 Hz, 2H), 4.10–4.02 (m, 1H), 1.57–1.44

(m, 1H), 1.34–1.29 (m, 2H), 0.86–0.81 (m, 6H); ^{13}C NMR (100 MHz, DMSO d_6): δ 169.8, 157.5, 156.2, 146.1, 137.2, 130.3, 130.2, 128.9, 128.2, 127.9, 124.4, 122.9, 121.1, 112.9, 69.8, 49.5, 48.7, 42.9, 35.3, 24.6, 23.2, 22.6; HRMS (AP-ESI) m/z calcd for $\text{C}_{24}\text{H}_{31}\text{N}_6\text{O}_4$ $[\text{M}+\text{H}]^+$ 467.2407, found 467.2403.

5.1.9.22. (S)-2-(3-((1-(3-(Benzyloxy)benzyl)-1H-1,2,3-triazol-4-yl)methyl)ureido)-N-hydroxy-4-methylpentanamide (**13w**). White solid, yield: 43%, mp: 154.7–156.1 °C. ^1H NMR (300 MHz, DMSO d_6): δ 10.66 (s, 1H), 8.78 (s, 1H), 7.89 (s, 1H), 7.45–7.25 (m, 6H), 6.98–6.96 (m, 2H), 6.86 (d, J = 7.5 Hz, 1H), 6.37 (t, J = 5.7 Hz, 1H), 6.11 (d, J = 8.7 Hz, 1H), 5.21 (s, 2H), 5.08 (s, 2H), 4.22 (d, J = 5.7 Hz, 2H), 4.10–4.02 (m, 1H), 1.55–1.44 (m, 1H), 1.34–1.30 (m, 2H), 0.86–0.82 (m, 6H); ^{13}C NMR (100 MHz, DMSO d_6): δ 169.8, 158.9, 157.6, 146.5, 138.0, 137.3, 130.3, 128.9, 128.3, 128.2, 122.9, 120.7, 115.1, 114.6, 69.7, 53.0, 49.5, 42.9, 35.4, 24.6, 23.2, 22.6; HRMS (AP-ESI) m/z calcd for $\text{C}_{24}\text{H}_{31}\text{N}_6\text{O}_4$ $[\text{M}+\text{H}]^+$ 467.2407, found 467.2417.

5.1.9.23. (S)-2-(3-((1-(2,6-Dichlorobenzyl)-1H-1,2,3-triazol-4-yl)methyl)ureido)-N-hydroxy-4-methylpentanamide (**13aa**). White solid, yield: 49%, mp: 184.8–186.4 °C. ^1H NMR (300 MHz, DMSO d_6): δ 10.66 (s, 1H), 8.78 (s, 1H), 7.80 (s, 1H), 7.58 (d, J = 8.1 Hz, 2H), 7.47 (t, J = 8.1 Hz, 1H), 6.35 (t, J = 5.4 Hz, 1H), 6.11 (d, J = 9.0 Hz, 1H), 5.76 (s, 2H), 4.20 (d, J = 5.4 Hz, 2H), 4.10–4.02 (m, 1H), 1.57–1.44 (m, 1H), 1.38–1.29 (m, 2H), 0.87–0.82 (m, 6H); ^{13}C NMR (100 MHz, DMSO d_6): δ 169.8, 157.5, 146.2, 136.3, 132.1, 130.8, 129.4, 122.9, 49.5, 48.9, 42.9, 35.3, 24.6, 23.2, 22.5; HRMS (AP-ESI) m/z calcd for $\text{C}_{17}\text{H}_{23}\text{Cl}_2\text{N}_6\text{O}_3$ $[\text{M}+\text{H}]^+$ 429.1209, found 429.1200.

5.1.9.24. (S)-2-(3-((1-(2,6-Dimethylbenzyl)-1H-1,2,3-triazol-4-yl)methyl)ureido)-N-hydroxy-4-methylpentanamide (**13bb**). White solid, yield: 55%, mp: 154.6–156.2 °C. ^1H NMR (300 MHz, DMSO d_6): δ 10.65 (s, 1H), 8.78 (s, 1H), 7.60 (s, 1H), 7.17 (t, J = 7.5 Hz, 1H), 7.08 (d, J = 7.5 Hz, 2H), 6.32 (t, J = 5.4 Hz, 1H), 6.09 (d, J = 9.0 Hz, 1H), 5.56 (s, 2H), 4.18 (d, J = 5.4 Hz, 2H), 4.09–4.04 (m, 1H), 2.33 (s, 6H), 1.56–1.43 (m, 1H), 1.33–1.28 (m, 2H), 0.87–0.81 (m, 6H); ^{13}C NMR (100 MHz, DMSO d_6): δ 169.8, 157.5, 146.1, 138.2, 132.1, 129.0, 128.9, 122.4, 49.4, 48.0, 42.9, 35.3, 24.6, 23.2, 22.5, 19.9; HRMS (AP-ESI) m/z calcd for $\text{C}_{19}\text{H}_{29}\text{N}_6\text{O}_3$ $[\text{M}+\text{H}]^+$ 389.2301, found 389.2308.

5.1.9.25. (S)-2-(3-((1-(2,6-Dimethoxybenzyl)-1H-1,2,3-triazol-4-yl)methyl)ureido)-N-hydroxy-4-methylpentanamide (**13cc**). White solid, yield: 52%, mp: 178.7–180.3 °C. ^1H NMR (300 MHz, DMSO d_6): δ 10.63 (s, 1H), 8.78 (s, 1H), 7.52 (s, 1H), 7.35 (t, J = 8.4 Hz, 1H), 6.72 (d, J = 8.4 Hz, 2H), 6.32 (t, J = 5.4 Hz, 1H), 6.09 (d, J = 9.0 Hz, 1H), 5.44 (s, 2H), 4.16 (d, J = 5.4 Hz, 2H), 4.09–4.01 (m, 1H), 3.81 (s, 6H), 1.54–1.43 (m, 1H), 1.33–1.29 (m, 2H), 0.87–0.81 (m, 6H); ^{13}C NMR (100 MHz, DMSO d_6): δ 169.8, 158.8, 157.5, 146.0, 131.2, 122.1, 110.9, 104.6, 56.4, 49.5, 42.8, 42.3, 35.3, 24.6, 23.2, 22.5; HRMS (AP-ESI) m/z calcd for $\text{C}_{19}\text{H}_{29}\text{N}_6\text{O}_5$ $[\text{M}+\text{H}]^+$ 421.2199, found 421.2207.

5.1.9.26. (S)-2-(3-((1-(3,4-Dichlorobenzyl)-1H-1,2,3-triazol-4-yl)methyl)ureido)-N-hydroxy-4-methylpentanamide (**13dd**). White solid, yield: 48%, mp: 178.7–180.3 °C. ^1H NMR (400 MHz, DMSO d_6): δ 10.68 (s, 1H), 8.78 (s, 1H), 7.88 (s, 1H), 7.70 (d, J = 4.0 Hz, 1H), 7.47 (dd, J = 8.0 Hz, J = 4.0 Hz, 1H), 7.25 (d, J = 8.0 Hz, 1H), 6.37 (t, J = 8.0 Hz, 1H), 6.12 (d, J = 8.0 Hz, 1H), 5.66 (s, 2H), 4.22 (d, J = 8.0 Hz, 2H), 4.10–4.03 (m, 1H), 1.54–1.45 (m, 1H), 1.34–1.30 (m, 2H), 0.87–0.82 (m, 6H); ^{13}C NMR (100 MHz, DMSO d_6): δ 169.8, 157.6, 146.5, 134.4, 134.1, 132.9, 132.3, 129.6, 128.3, 123.3, 50.3, 49.5, 42.9, 42.3, 35.3, 24.6, 23.2, 22.6; HRMS

(AP-ESI) m/z calcd for $\text{C}_{17}\text{H}_{23}\text{Cl}_2\text{N}_6\text{O}_3$ $[\text{M}+\text{H}]^+$ 429.1209, found 429.1215.

5.1.9.27. (S)-2-(3-((1-(3,4-Dimethoxybenzyl)-1H-1,2,3-triazol-4-yl)methyl)ureido)-N-hydroxy-4-methylpentanamide (**13ee**). White solid, yield: 53%, mp: 160.8–162.5 °C. ^1H NMR (300 MHz, DMSO d_6): δ 10.67 (s, 1H), 8.80 (s, 1H), 7.86 (s, 1H), 7.00 (s, 1H), 6.93 (d, J = 8.4 Hz, 1H), 6.86 (d, J = 8.4 Hz, 1H), 6.40 (t, J = 5.4 Hz, 1H), 6.15 (d, J = 9.0 Hz, 1H), 5.45 (s, 2H), 4.19 (d, J = 5.4 Hz, 2H), 4.09–4.01 (m, 1H), 3.73 (s, 6H), 1.54–1.43 (m, 1H), 1.34–1.29 (m, 2H), 0.86–0.81 (m, 6H); ^{13}C NMR (100 MHz, DMSO d_6): δ 169.8, 157.6, 149.2, 149.1, 146.5, 128.7, 122.6, 121.1, 112.5, 112.3, 56.0, 55.9, 53.0, 49.6, 42.8, 35.4, 24.6, 23.2, 22.5; HRMS (AP-ESI) m/z calcd for $\text{C}_{19}\text{H}_{29}\text{N}_6\text{O}_5$ $[\text{M}+\text{H}]^+$ 421.2199, found 421.2203.

5.1.9.28. (S)-N-hydroxy-4-methyl-2-(3-((1-(3,4,5-trimethoxybenzyl)-1H-1,2,3-triazol-4-yl)methyl)ureido)pentanamide (**13ff**). White solid, yield: 56%, mp: 152.9–154.2 °C. ^1H NMR (300 MHz, DMSO d_6): δ 10.67 (s, 1H), 8.80 (s, 1H), 7.90 (s, 1H), 6.69 (s, 2H), 6.37 (t, J = 5.4 Hz, 1H), 6.12 (d, J = 9.0 Hz, 1H), 5.46 (s, 2H), 4.21 (d, J = 5.4 Hz, 2H), 4.09–4.01 (m, 1H), 3.75 (s, 6H), 3.63 (s, 3H), 1.57–1.43 (m, 1H), 1.34–1.29 (m, 2H), 0.86–0.81 (m, 6H); ^{13}C NMR (100 MHz, DMSO d_6): δ 169.8, 161.1, 157.5, 153.4, 146.5, 137.7, 131.8, 122.8, 106.5, 106.1, 60.4, 56.3, 55.6, 53.4, 49.5, 42.9, 35.3, 24.6, 23.1, 22.5; HRMS (AP-ESI) m/z calcd for $\text{C}_{20}\text{H}_{31}\text{N}_6\text{O}_6$ $[\text{M}+\text{H}]^+$ 451.2305, found 451.2311.

5.1.9.29. (2S,3R)-2-(3-((1-Benzyl-1H-1,2,3-triazol-4-yl)methyl)ureido)-N-hydroxy-3-methylpentanamide (**14**). White solid, yield: 58%, mp: 176.9–178.6 °C. ^1H NMR (600 MHz, DMSO d_6): δ 10.60 (s, 1H), 8.78 (s, 1H), 7.90 (s, 1H), 7.40–7.29 (m, 5H), 6.47–6.40 (m, 1H), 6.16–6.08 (m, 1H), 5.56 (s, 2H), 4.28–4.15 (m, 2H), 4.03–3.83 (m, 1H), 1.61–1.23 (m, 2H), 1.07–0.92 (m, 1H), 0.85–0.83 (m, 6H); ^{13}C NMR (100 MHz, DMSO d_6): δ 169.2, 157.9, 146.5, 136.5, 129.1, 128.5, 128.3, 122.9, 55.2, 54.5, 53.1, 38.2, 35.4, 26.1, 24.9; HRMS (AP-ESI) m/z calcd for $\text{C}_{17}\text{H}_{25}\text{N}_6\text{O}_3$ $[\text{M}+\text{H}]^+$ 361.1988, found 361.2005.

5.1.9.30. (S)-2-(3-((1-(4-Chlorobenzyl)-1H-1,2,3-triazol-4-yl)methyl)ureido)-N-hydroxy-2-phenylacetamide (**15**). White solid, yield: 65%, mp: 202.4–204.2 °C. ^1H NMR (400 MHz, DMSO d_6): δ 11.00 (s, 1H), 9.00 (s, 1H), 7.92 (s, 1H), 7.44 (d, J = 8.4 Hz, 2H), 7.37–7.30 (m, 6H), 7.28–7.23 (m, 1H), 6.89 (d, J = 8.7 Hz, 1H), 6.65 (t, J = 5.7 Hz, 1H), 5.56 (s, 2H), 5.19 (d, J = 8.7 Hz, 1H), 4.28–4.17 (m, 2H); ^{13}C NMR (100 MHz, DMSO d_6): δ 167.7, 157.3, 146.6, 140.6, 135.5, 133.3, 130.3, 129.2, 128.7, 127.8, 126.9, 123.0, 54.7, 52.4, 35.4; HRMS (AP-ESI) m/z calcd for $\text{C}_{19}\text{H}_{22}\text{ClN}_6\text{O}_3$ $[\text{M}+\text{H}]^+$ 415.1285, found 415.1282.

5.1.9.31. (S)-2-(3-((1-(2-Aminobenzyl)-1H-1,2,3-triazol-4-yl)methyl)ureido)-N-hydroxy-4-methylpentanamide (**20a**). White solid, yield: 30%, mp: 142.6–144.3 °C. ^1H NMR (600 MHz, DMSO d_6): δ 10.66 (s, 1H), 8.78 (s, 1H), 7.79 (s, 1H), 7.03 (t, J = 7.8 Hz, 1H), 6.94 (d, J = 7.8 Hz, 1H), 6.67 (d, J = 7.8 Hz, 1H), 6.53 (t, J = 7.8 Hz, 1H), 6.36 (t, J = 5.4 Hz, 1H), 6.10 (d, J = 9 Hz, 1H), 5.42 (s, 2H), 5.23 (s, 2H), 4.21–4.20 (m, 2H), 4.07–4.04 (m, 1H), 1.51–1.48 (m, 1H), 1.32–1.30 (m, 2H), 0.86–0.83 (m, 6H); ^{13}C NMR (100 MHz, DMSO d_6): δ 169.8, 157.5, 147.0, 146.3, 130.3, 129.6, 122.8, 119.3, 116.7, 115.8, 50.0, 49.5, 42.9, 35.3, 24.6, 23.2, 22.6; HRMS (AP-ESI) m/z calcd for $\text{C}_{17}\text{H}_{26}\text{N}_7\text{O}_3$ $[\text{M}+\text{H}]^+$ 376.2097, found 376.2102.

5.1.9.32. (S)-2-(3-((1-(3-Aminobenzyl)-1H-1,2,3-triazol-4-yl)methyl)ureido)-N-hydroxy-4-methylpentanamide (**20b**). White solid, yield: 23%, mp: 88.9–90.2 °C. ^1H NMR (600 MHz, DMSO d_6): δ 10.66 (s, 1H), 8.79 (s, 1H), 7.81 (s, 1H), 6.98 (t, J = 7.8 Hz, 1H), 6.48 (d, J = 7.8 Hz, 1H), 6.44 (s, 1H), 6.41 (d, J = 7.8 Hz, 1H), 6.34 (t, J = 5.4 Hz,

1H), 6.11 (d, J = 9.0 Hz, 1H), 5.36 (s, 2H), 5.15 (s, 2H), 4.21–4.17 (m, 2H), 4.07–4.03 (m, 1H), 1.52–1.48 (m, 1H), 1.33–1.30 (m, 2H), 0.86–0.83 (m, 6H); ^{13}C NMR (100 MHz, DMSO- d_6): δ 169.8, 157.6, 149.4, 146.4, 136.9, 129.6, 122.8, 115.5, 114.0, 113.4, 53.5, 49.6, 42.8, 35.4, 24.6, 23.2, 22.6; HRMS (AP-ESI) m/z calcd for $\text{C}_{17}\text{H}_{27}\text{N}_7\text{O}_3$ $[\text{M}+\text{H}]^+$ 376.2097, found 376.2091.

5.1.9.33. (*S,E*)-2-(3-((1-Cinnamyl-1H-1,2,3-triazol-4-yl)methyl)ureido)-N-hydroxy-4-methylpentanamide (**25a**). White solid, yield: 45%, mp: 178.9–180.5 °C. ^1H NMR (300 MHz, DMSO d_6): δ 10.66 (s, 1H), 8.79 (s, 1H), 7.88 (s, 1H), 7.47–7.45 (m, 2H), 7.37–7.25 (m, 3H), 6.66 (d, J = 15.9 Hz, 1H), 6.48 (d, J = 15.9 Hz, 1H), 6.39 (t, J = 5.4 Hz, 1H), 6.13 (d, J = 8.7 Hz, 1H), 5.14 (d, J = 6.3 Hz, 2H), 4.23 (d, J = 5.4 Hz, 2H), 4.10–4.02 (m, 1H), 1.57–1.42 (m, 1H), 1.34–1.30 (m, 2H), 0.86–0.82 (m, 6H); ^{13}C NMR (100 MHz, DMSO d_6): δ 169.8, 157.6, 146.5, 136.2, 134.1, 129.1, 128.5, 127.0, 124.1, 122.7, 51.7, 49.5, 42.9, 35.4, 24.6, 23.2, 22.6; HRMS (AP-ESI) m/z calcd for $\text{C}_{19}\text{H}_{27}\text{N}_6\text{O}_3$ $[\text{M}+\text{H}]^+$ 387.2145, found 387.2146.

5.1.9.34. (*S*)-N-hydroxy-4-methyl-2-(3-((1-phenethyl-1H-1,2,3-triazol-4-yl)methyl)ureido)pentanamide (**25b**). White solid, yield: 41%, mp: 178.4–180.1 °C. ^1H NMR (300 MHz, DMSO d_6): δ 10.69 (s, 1H), 8.82 (s, 1H), 7.83 (s, 1H), 7.31–7.19 (m, 5H), 6.36 (t, J = 5.4 Hz, 1H), 6.14 (d, J = 9.0 Hz, 1H), 4.57 (d, J = 7.5 Hz, 2H), 4.20 (d, J = 5.4 Hz, 2H), 4.11–4.03 (m, 1H), 3.13 (d, J = 7.5 Hz, 2H), 1.57–1.46 (m, 1H), 1.36–1.31 (m, 2H), 0.89–0.84 (m, 6H); ^{13}C NMR (100 MHz, DMSO d_6): δ 169.8, 157.6, 146.0, 138.1, 129.1, 128.8, 127.0, 122.8, 50.7, 49.6, 42.9, 36.2, 35.3, 24.6, 23.2, 22.6; HRMS (AP-ESI) m/z calcd for $\text{C}_{18}\text{H}_{27}\text{N}_6\text{O}_3$ $[\text{M}+\text{H}]^+$ 375.2145, found 375.2159.

5.1.9.35. (*S*)-N-hydroxy-4-methyl-2-(3-((1-(pyridin-3-ylmethyl)-1H-1,2,3-triazol-4-yl)methyl)ureido)pentanamide (**25c**). White solid, yield: 49%, mp: 144.6–146.3 °C. ^1H NMR (600 MHz, DMSO d_6): δ 10.66 (s, 1H), 8.80 (s, 1H), 8.58 (s, 1H), 8.55–8.54 (m, 1H), 7.97 (s, 1H), 7.72–7.70 (m, 1H), 7.41–7.39 (m, 1H), 6.37 (t, J = 5.4 Hz, 1H), 6.11 (d, J = 9.0 Hz, 1H), 5.62 (s, 2H), 4.21 (d, J = 5.4 Hz, 2H), 4.07–4.03 (m, 1H), 1.51–1.48 (m, 1H), 1.33–1.30 (m, 2H), 0.86–0.83 (m, 6H); ^{13}C NMR (100 MHz, DMSO d_6): δ 169.8, 157.6, 149.8, 149.6, 146.7, 136.2, 132.2, 124.2, 123.0, 50.6, 49.5, 42.9, 35.4, 24.6, 23.2, 22.6; HRMS (AP-ESI) m/z calcd for $\text{C}_{16}\text{H}_{24}\text{N}_7\text{O}_3$ $[\text{M}+\text{H}]^+$ 362.1941, found 362.1940.

5.1.9.36. (*S*)-N-hydroxy-4-methyl-2-(3-((1-(naphthalen-1-ylmethyl)-1H-1,2,3-triazol-4-yl)methyl)ureido)pentanamide (**25d**). White solid, yield: 46%, mp: 178.5–180.2 °C. ^1H NMR (300 MHz, DMSO d_6): δ 10.66 (s, 1H), 8.79 (s, 1H), 8.21–8.18 (m, 1H), 8.00–7.94 (m, 2H), 7.83 (s, 1H), 7.62–7.48 (m, 3H), 7.44–7.42 (m, 1H), 6.34 (t, J = 5.4 Hz, 1H), 6.09 (d, J = 9.0 Hz, 1H), 6.06 (s, 2H), 4.18 (d, J = 5.4 Hz, 2H), 4.07–4.00 (m, 1H), 1.52–1.43 (m, 1H), 1.32–1.27 (m, 2H), 0.85–0.80 (m, 6H); ^{13}C NMR (100 MHz, DMSO d_6): δ 169.8, 157.5, 146.5, 133.8, 132.0, 131.1, 129.4, 129.1, 127.7, 127.2, 126.6, 126.0, 123.7, 123.0, 51.1, 49.5, 42.8, 35.3, 24.6, 23.2, 22.5; HRMS (AP-ESI) m/z calcd for $\text{C}_{21}\text{H}_{27}\text{N}_6\text{O}_3$ $[\text{M}+\text{H}]^+$ 411.2145, found 411.2150.

5.1.9.37. (*S*)-N-hydroxy-4-methyl-2-(3-((1-(naphthalen-2-ylmethyl)-1H-1,2,3-triazol-4-yl)methyl)ureido)pentanamide (**25e**). White solid, yield: 51%, mp: 174.8–176.4 °C. ^1H NMR (600 MHz, DMSO d_6): δ 10.65 (s, 1H), 8.78 (s, 1H), 7.94–7.90 (m, 4H), 7.86 (s, 1H), 7.57–7.51 (m, 2H), 7.45–7.41 (m, 1H), 6.36 (t, J = 5.4 Hz, 1H), 6.10 (d, J = 8.7 Hz, 1H), 5.73 (s, 2H), 4.22 (d, J = 5.4 Hz, 2H), 4.08–4.00 (m, 1H), 1.53–1.44 (m, 1H), 1.33–1.28 (m, 2H), 0.84–0.80 (m, 6H); ^{13}C NMR (100 MHz, DMSO d_6): δ 169.8, 157.5, 146.6, 134.0, 133.2, 132.9, 128.9, 128.2, 128.0, 127.4, 127.0, 126.8, 126.2, 123.0, 53.3, 49.5, 42.8, 35.4, 24.6, 23.1, 22.5; HRMS

(AP-ESI) m/z calcd for $\text{C}_{21}\text{H}_{27}\text{N}_6\text{O}_3$ $[\text{M}+\text{H}]^+$ 411.2145, found 411.2154.

5.1.9.38. (2*S*)-N-hydroxy-4-methyl-2-(3-((1-(1-phenylethyl)-1H-1,2,3-triazol-4-yl)methyl)ureido)pentanamide (**25f**). White solid, yield: 49%, mp: 110.7–112.6 °C. ^1H NMR (400 MHz, DMSO d_6): δ 10.56 (s, 1H), 8.79 (s, 1H), 7.96 (s, 1H), 7.39–7.30 (m, 5H), 6.35 (t, J = 8.0 Hz, 1H), 6.10 (d, J = 8.0 Hz, 1H), 5.91 (q, J = 8.0 Hz, 1H), 4.21 (d, J = 8.0 Hz, 2H), 4.09–4.03 (m, 1H), 1.86 (d, J = 8.0 Hz, 3H), 1.56–1.48 (m, 1H), 1.34–1.30 (m, 2H), 0.88–0.83 (m, 6H); ^{13}C NMR (100 MHz, DMSO d_6): δ 169.8, 157.6, 146.2, 141.4, 129.1, 128.4, 126.8, 121.6, 59.5, 49.5, 42.8, 35.4, 24.6, 23.2, 22.6, 21.4; HRMS (AP-ESI) m/z calcd for $\text{C}_{18}\text{H}_{27}\text{N}_6\text{O}_3$ $[\text{M}+\text{H}]^+$ 375.2145, found 375.2156.

5.1.9.39. (2*S*)-N-hydroxy-2-(3-((1-(2-methoxyphenyl)ethyl)-1H-1,2,3-triazol-4-yl)methyl)ureido)-4-methylpentanamide (**25g**). White solid, yield: 41%, mp: 142.5–144.1 °C. ^1H NMR (300 MHz, DMSO d_6): δ 10.65 (s, 1H), 8.78 (s, 1H), 7.86 (s, 1H), 7.31 (t, J = 8.7 Hz, 1H), 7.06 (t, J = 8.7 Hz, 2H), 6.94 (t, J = 8.7 Hz, 1H), 6.34 (t, J = 5.4 Hz, 1H), 6.12 (q, J = 6.9 Hz, 1H), 6.10 (d, J = 9.0 Hz, 1H), 4.21 (d, J = 5.4 Hz, 2H), 4.10–4.02 (m, 1H), 3.81 (s, 3H), 1.80 (d, J = 6.9 Hz, 3H), 1.55–1.47 (m, 1H), 1.34–1.29 (m, 2H), 0.87–0.82 (m, 6H); ^{13}C NMR (100 MHz, DMSO d_6): δ 169.8, 157.6, 156.3, 145.8, 129.8, 129.0, 126.9, 121.9, 121.0, 111.8, 56.1, 53.9, 49.5, 42.8, 35.4, 24.6, 23.2, 22.5, 20.7; HRMS (AP-ESI) m/z calcd for $\text{C}_{19}\text{H}_{29}\text{N}_6\text{O}_4$ $[\text{M}+\text{H}]^+$ 405.2250, found 405.2257.

5.1.9.40. (*S*)-2-(3-((1-Benzhydryl-1H-1,2,3-triazol-4-yl)methyl)ureido)-N-hydroxy-4-methylpentanamide (**25h**). White solid, yield: 40%, mp: 178.4–180.3 °C. ^1H NMR (400 MHz, DMSO d_6): δ 10.67 (s, 1H), 8.79 (s, 1H), 7.83 (s, 1H), 7.42–7.33 (m, 6H), 7.28 (s, 1H), 7.21–7.19 (m, 4H), 6.38 (t, J = 8.0 Hz, 1H), 6.11 (d, J = 8.0 Hz, 1H), 4.24 (d, J = 8.0 Hz, 2H), 4.09–4.03 (m, 1H), 1.55–1.43 (m, 1H), 1.33–1.30 (m, 2H), 0.87–0.81 (m, 6H); ^{13}C NMR (100 MHz, DMSO d_6): δ 169.8, 157.5, 146.7, 146.6, 139.2, 136.5, 131.4, 131.4, 131.1, 129.2, 128.5, 128.4, 127.5, 123.1, 122.9, 122.2, 52.3, 49.5, 42.9, 35.3, 24.6, 23.2, 22.6; HRMS (AP-ESI) m/z calcd for $\text{C}_{23}\text{H}_{29}\text{N}_6\text{O}_3$ $[\text{M}+\text{H}]^+$ 437.2301, found 437.2300.

5.2. Biological evaluation

5.2.1. APN inhibition assay

IC_{50} values against APN were determined by using L-Leu-*p*-nitroanilide as substrate and microsomal APN from porcine kidney microsomes (Biocol) in 50 mM PBS, pH 7.2 as enzyme. The inhibitors (40 μL) at various concentrations were incubated with APN (10 μL) at 37 °C for 5 min. Then, substrate (5 μL) was added to the above solution and PBS was added to adjust the assay mixture to 200 μL . The mixture was incubated at 37 °C for another 30 min. The hydrolysis product *p*-nitroanilide was measured according to the absorbance monitored at 405 nm with a plate reader (Varioskan, Thermo, USA).

5.2.2. Enzyme inhibition assay towards APN from ES-2 or PLC/PRF/5 cells

IC_{50} values against APN were determined by using L-Leu-*p*-nitroanilide as substrate and APN on the surface of ES-2 cells or PLC/PRF/5 cells in 10 mM PBS, pH 7.4 as enzyme. The inhibitors (20 μL) were incubated with ES-2 cells or PLC/PRF/5 cells (70 μL , $2.8 \times 10^6/\text{mL}$) at 37 °C for 5 min. Then, substrate (10 μL) and $1 \times$ PBS buffer (100 μL) was added to the above solution. The mixture was incubated at 37 °C for 1 h. After centrifugation, the hydrolysis product *p*-nitroanilide in the supernatant was monitored at 405 nm with a plate reader (Varioskan, Thermo, USA).

5.2.3. Anti-proliferation assay

Anti-proliferation abilities of compounds were evaluated by the MTT [(3-[4,5-dimethyl-2-thiazolyl]-2,5-diphenyl-2H-tetrazolium bromide)] method. Cells were grown in RPMI 1640 medium with 10% FBS at 37 °C in 5% CO₂ humidified incubator. In brief, cells (100 µL) were plated in 96-well plates and cultivated for 4 h, and then treated with different concentrations of inhibitors (100 µL) for 48 h. MTT (20 µL, 5 mg/mL) solution was added into the test well. After incubation for another 4 h, DMSO (200 µL) was added and mixed for 15 min to extract the formed formazan from MTT. The optical density was then measured using a plate reader at 570 nm (Varioskan, Thermo, USA).

5.2.4. HUVEC tubular structure formation assay

Matrigel (50 µL; BD biosciences) was added into test well of 96-well plates and then allowed to polymerize for 0.5 h at 37 °C. HUVECs (20,000 cells/well) in M199 medium (50 µL) and inhibitors (50 µL) at the specified concentrations were added and incubated at 37 °C in 5% CO₂ for 4 h. Images of five random fields per well were analyzed by Motic Image Plus 2.0 software (Motic Instruments Inc., Canada). The numbers of branch points of the formed tubes were counted and the average numbers were calculated. Experiments were repeated three times.

5.2.5. Rat aortic ring assay

Matrigel (100 µL; BD bioscience) was added into 96-well plates and then allowed to polymerize for 0.5 h at 37 °C. The thoracic aortas were separated from 8- to 10-week-old male Sprague Dawley rats. After careful removal of fibroadipose tissues, the aortas were cut into 1-mm-long cross-section. The aortas fragments were placed into test well of 96-well plates and then covered with an additional 100 µL of matrigel. After incubation at 37 °C and 5% CO₂ for 0.5 h, the matrigel solidified. The aortas rings were treated with inhibitors at 37 °C in 5% CO₂ for 9 days. The micro-vessels formed and were visualized by inverted microscope at 100× magnification. The culture medium containing inhibitors was changed every three days. The quantity of assay is valued by relative area covered with microvessels using Image-pro Plus 6.0.²⁷ Experiments were repeated three times using aortas from four different rats.

5.2.6. In vivo mouse H22 pulmonary metastasis model

All experiments involving laboratory animals were performed with the approval of the local ethics committee. The mouse hepatoma H22 cell line was obtained from Dr. Jia (Shandong Academy of Medical Sciences, China) as a kind gift. 6-week old male Kunming mice were purchased from Center for New Drugs Evaluation of Shandong University, China. To establish a H22 pulmonary metastasis model, H22 cells (7.5×10^6) were suspended in 0.1 mL of PBS and were injected *via* tail vein on day one. Mice were randomly divided into treatment and control group. The treatment groups received 60 mg/kg/d of compounds intraperitoneally, the control group received an equal volume of PBS intraperitoneally, from day 1 to day 12. The body weight was monitored every two days. One day 13, animals were sacrificed and the lungs were removed and fixed in Bouin's solution. The metastasis nodes on the surface of pulmonary lobes were counted.

5.3. Molecular docking studies

Compound **13v** and **13a** were docked into the active site of APN (PDB code: 2DQM) using Sybyl_X 1.3. The residues in a 10.0 Å radius circles around bestatin in the co-crystal structure (PDB code: 2DQM) were selected as the active site. Before docking studies, the protein structure was treated by deleting water molecules, adding hydrogen atoms, modifying atom types, and assigning with AMBER7 FF99 charges. A 100-step minimization process was per-

formed to further optimize the protein structure. The molecular structures were generated with Sybyl/Sketch module and optimized using Powell's method with the Tripos force field with convergence criterion set at 0.05 kcal/Å mol and assigned with the Gasteiger-Hückel method. Molecular docking was carried out *via* the Sybyl/Surflex-Dock module. Other docking parameters implied in the program were default values. The top-scoring pose was selected for discussions.

5.4. Statistical analysis

The statistical significance of differences between the groups was assessed by Student's *t* test. *P* < 0.05 was considered as statistically significant.

Acknowledgements

This work was supported by Natural Science Foundation of Shandong Province (Grant No. ZR2018QH007), National Natural Science Foundation of China (Grant No. 81373282), Major Project of Science and Technology of Shandong Province (Grant No. 2015ZDJS04001, 2017CXGC1401), Young Scholars Program of Shandong University (YSPSDU, Grant No. 2016WLJH33).

Conflict of interest

The authors confirm that this article content has no conflict of interest.

A. Supplementary data

Supplementary data associated with this article can be found, in the online version, at <https://doi.org/10.1016/j.bmc.2018.04.041>.

References

- Look AT, Ashmun RA, Shapiro LH, Peiper SC. *J Clin Invest*. 1989;83:1299.
- Hooper NM. *FEBS Lett*. 1994;354:1.
- Tokuhara T, Hattori N, Ishida H, et al. *Clin Cancer Res*. 2006;12:3971.
- Saiki I, Murata J, Watanabe K, Fujii H, Abe F, Azuma I. *Jpn J Cancer Res*. 1989;80:873.
- Yoneda J, Saiki I, Fujii H, Abe F, Kojima Y, Azuma I. *Clin Exp Metastasis*. 1992;10:49.
- Saiki I, Fujii H, Yoneda J, et al. *Int J Cancer*. 1993;54:137.
- Fujii H, Nakajima M, Saiki I, Yoneda J, Azuma I, Tsuruo T. *Clin Exp Metastasis*. 1995;13:337.
- Aozuka Y, Koizumi K, Saitoh Y, Ueda Y, Sakurai H, Saiki I. *Cancer Lett*. 2004;216:35.
- Guzman-Rojas L, Rangel R, Salameh A, et al. *Proc Natl Acad Sci USA*. 2012;109:1637.
- Umezawa H, Aoyagi T, Suda H, Hamada M, Takeuchi T. *J Antibiot*. 1976;29:97.
- Rich DH, Moon BJ, Harbeson S. *J Med Chem*. 1984;27:417.
- Umezawa H, Aoyagi T, Tanaka T, et al. *J Antibiot*. 1985;38:1629.
- Nagai M, Kojima F, Naganawa H, Hamada M, Aoyagi T, Takeuchi T. *J Antibiot*. 1997;50:82.
- Repic Lampret B, Kidric J, Kralj B, Vitale L, Pokorny M, Renko M. *Arch Microbiol*. 1999;171:397.
- Jiang Y, Li X, Hou J, et al. *Eur J Med Chem*. 2018;143:334.
- Jiang Y, Hou J, Li X, et al. *Bioorg Med Chem*. 2016;24:5787.
- Jiang Y, Li X, Hou J, et al. *Eur J Med Chem*. 2016;121:649.
- Su L, Jia YP, Wang XJ, Zhang L, Fang H, Xu WF. *Bioorg Med Chem Lett*. 2013;23:2512.
- Su L, Cao JY, Jia YP, Zhang XN, Fang H, Xu WF. *ACS Med Chem Lett*. 2012;3:959.
- Ma C, Cao J, Liang X, et al. *Eur J Med Chem*. 2016;108:21.
- Ma C, Jin K, Cao J, Zhang L, Li X, Xu W. *Bioorg Med Chem*. 2013;21:1621.
- Tron GC, Pirali T, Billington RA, Canonico PL, Sorba G, Genazzani AA. *Med Res Rev*. 2008;28:278.
- Musumeci F, Schenone S, Desogus A, Nieddu E, Deodato D, Botta L. *Curr Med Chem*. 2015;22:2022.
- Thirumurugan P, Matosiuk D, Jozwiak K. *Chem Rev*. 2013;113:4905.
- Barlow Th MA, Tourwé D, Ballet S. *Eur J Org Chem*. 2017;2017:4678.
- Peheré AD, Zhang X, Abell AD. *Aust J Chem*. 2017;70:138.
- Blatt RJ, Clark AN, Courtney J, Tully C, Tucker AL. *Comput Methods Programs Biomed*. 2004;75:75.